

# Quantum Computing Hardware Platforms: Superconducting Transmon Machines

- CSC591/ECE592 – Quantum Computing
  - Fall 2020
    - Professor Patrick Dreher
- Research Professor, Department of Computer Science
  - Chief Scientist, NC State IBM Q Hub

# Outline

- Introduction – Digital versus Quantum Computation
- Conceptual design for superconducting transmon QC hardware platforms
  - Construction of qubits with electronic circuits
  - Superconductivity
  - Josephson junction and nonlinear LC circuits
  - Transmon design with example IBM chip layout
- Working with a superconducting transmon hardware platform
  - Quantum Mechanics of Two State Systems - Rabi oscillations
  - Performance characteristics of superconducting transmon hardware
  - Construct the basic CNOT gate
  - Entangled transmons and controlled gates
- Appendices
  - References
  - Quantum mechanical solution of the 2 level system

# Digital Computation Hardware Platforms Based on a Base<sub>2</sub> Mathematics

- Design principle for a digital computer is built on base<sub>2</sub> mathematics
- Identify voltage changes in electrical circuits that map base<sub>2</sub> math into a “zero” or “one” corresponding to an on/off state
- Build electrical circuits from simple on/off states that apply these basic rules to construct digital computers

## From Previous Lectures

It was shown that basic digital electronic gates (ex. NAND etc.) are inconsistent as design primitives for constructing a quantum computer

So if it is known that standard NAND digital logic circuits can't reproduce the proper quantum mechanical behavior as summarized in the axioms of quantum mechanics how is a gate based quantum computer hardware designed and constructed?

## Question:

How can one construct a physical piece of hardware that operates in a manner that emulates quantum mechanical behavior as described by the axioms of quantum mechanics?

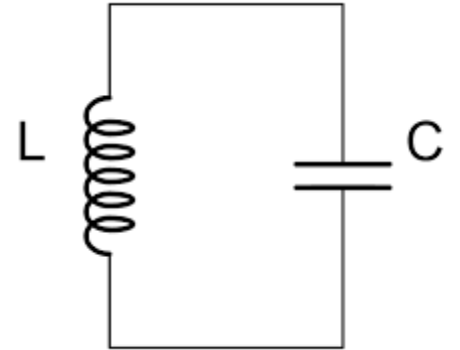
# Conceptual Design Requirements for a Gate-based Superconducting Transmon Quantum Computer

- The hardware design must incorporate the ability to
  - Construct a physical system with (at least) two uniquely addressable quantum mechanical states
  - Initialize the state of those qubits
  - Implement arbitrary rotations of the qubit's state on the Bloch sphere
  - Construct a set of universal gates
  - Entangle two qubits
  - Design a hardware platform that operates with
    - Decoherence times sufficiently long to implement a circuit with enough depth to accomplish a calculation
    - A way to measure the final output state of the qubits

# Consider and LC Resonant Circuit

- In classical linear circuit theory, the natural solution for the current in an LC circuit is

$$i(t) = I_0 \cos \omega_0 t, \quad \omega_0 = 1 / \sqrt{LC}$$



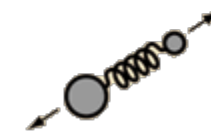
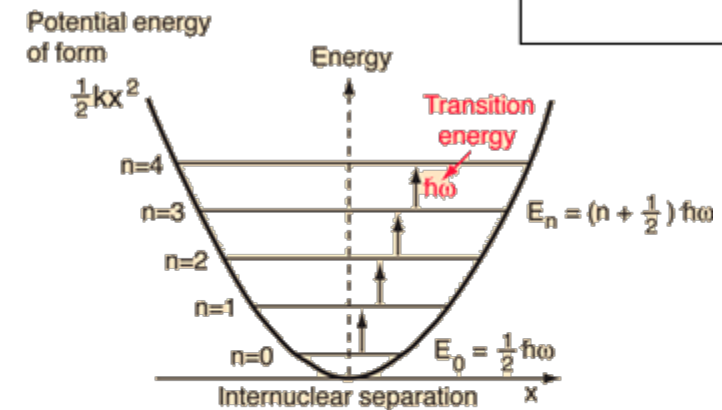
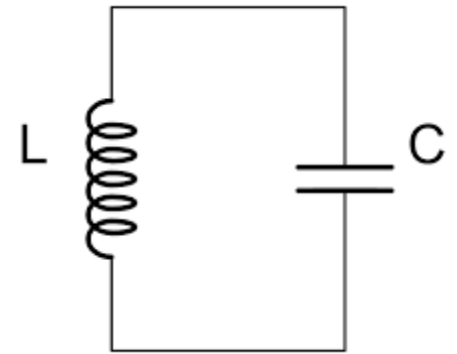
- The current can have any amplitude, independent of the frequency
- Energy is stored alternately in the electric field of the capacitor and the magnetic field of the inductor and can have any value at room temperature  $U_0 \sim I^2$
- Circuit creates an oscillatory behavior

# Analogy of LC Circuit at Low Temperature to Harmonic Oscillator Energy Levels

- If the LC circuit is cooled to a superconducting temperature (less than 4° K) then the circuit will begin to display equally spaced quantized energy levels

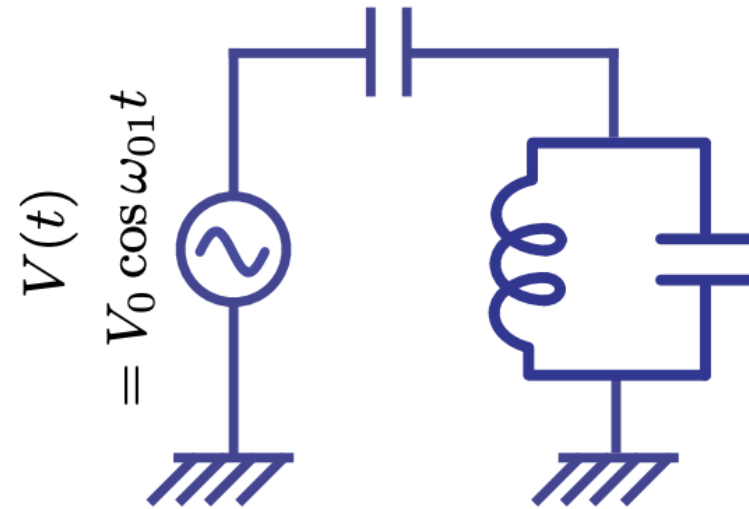
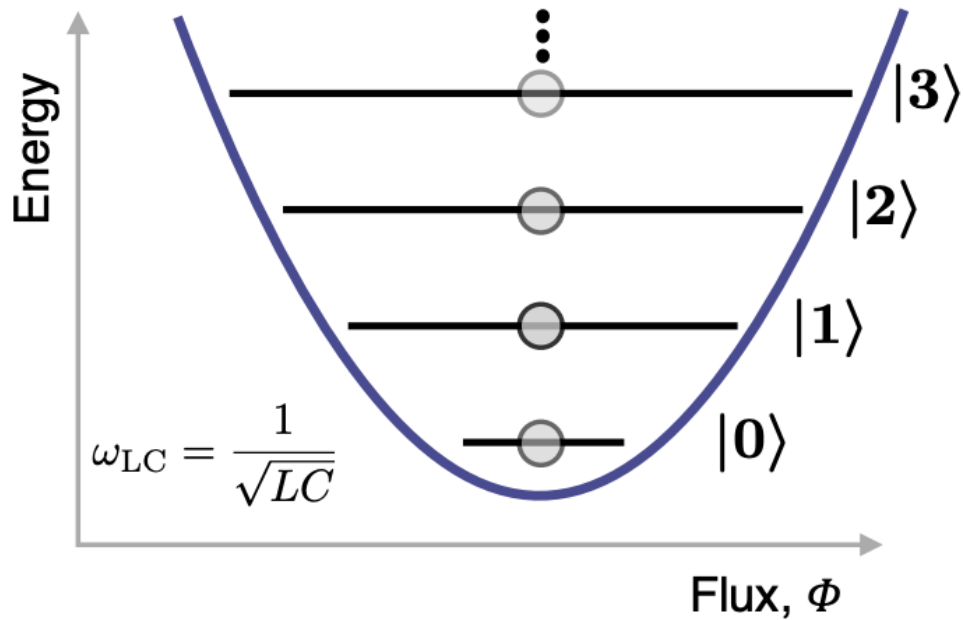
$$U = \hbar\omega_0 \left( n + \frac{1}{2} \right)$$

- This construct provides discrete states



x=0 represents the equilibrium separation between the nuclei.

# Propose Assigning Qubits to LC Resonant Circuit Energy Levels



# Mapping Qubits to LC Circuit Energy Levels

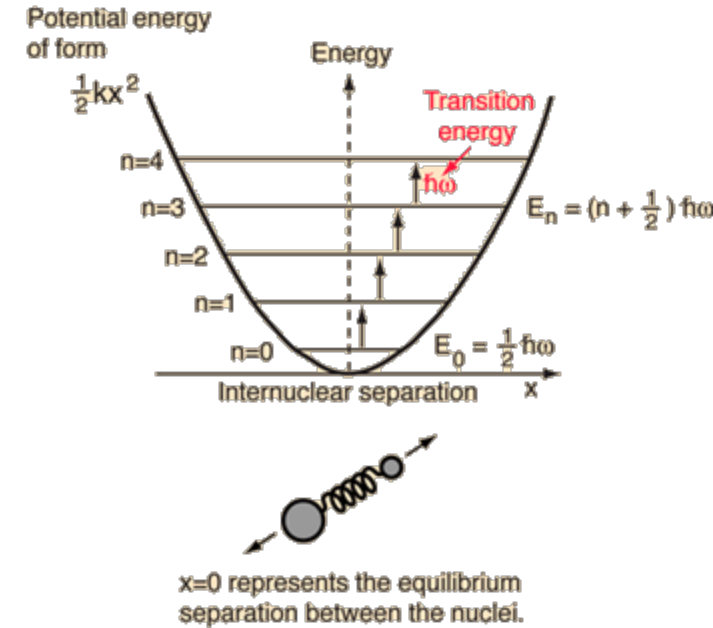
- Difficulty is that all of the discrete states are equidistant in energy (i.e. energy difference between 0 state and the 1 state is the same as energy difference between all other states  $n, n+1$ )
- Impossible to distinguish a  $|0\rangle$  state from a  $|1\rangle$  state
- Need to construct a mechanism to be able to make this distinction

# Potential Solution

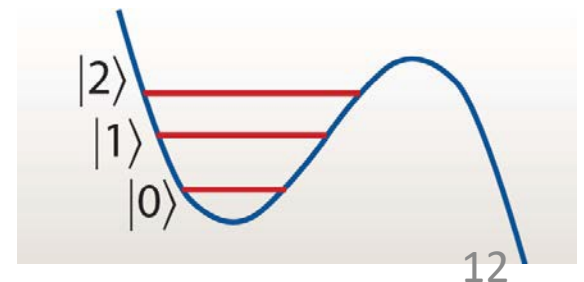
- If there was some way to set the levels such that their values depended on the magnitude of the current or voltage, then the energy levels would no longer be equally spaced!

# Nonlinear LC Circuits

- If a nonlinearity could be introduced into the harmonic oscillator energy levels in a way that the energy difference between  $n=0$  and  $n=1$  was different from the energy difference from all other states, it will be possible to selectively address each particular transition by tuning the frequency of the applied excitation



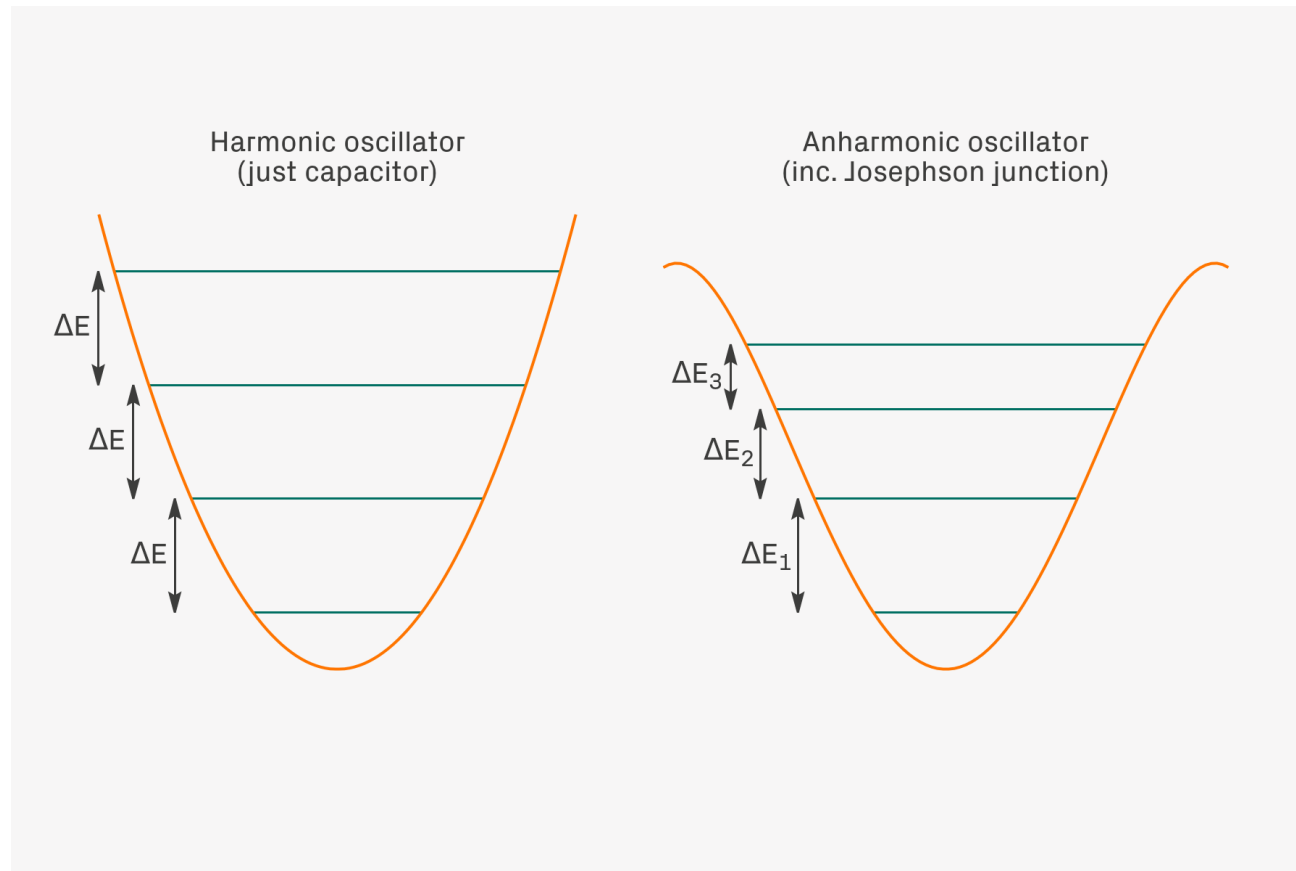
Graphic: <http://hyperphysics.phy-astr.gsu.edu/hbase/quantum/hosc.html>



Graphic: Clarke & Wilhelm

# Energy Level Comparison

## Harmonic versus Anharmonic Oscillator



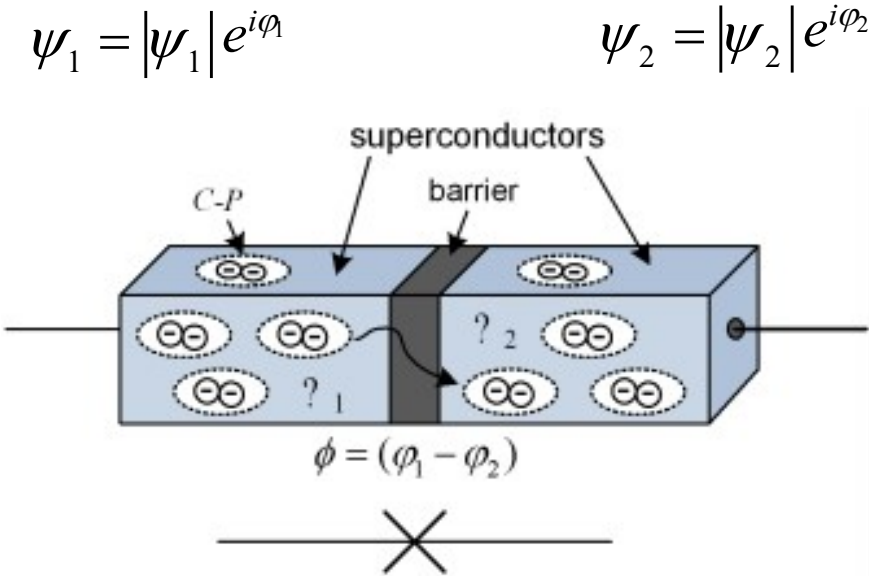
3 November 2020  
5 November 2020

Superconducting Transmon Quantum Computers  
Patrick Dreher

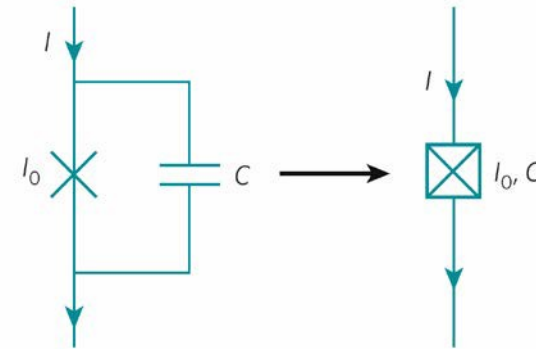
# What Types of Materials Work at these Extreme Low Temperatures

- At these low temperatures, metals such as aluminum (Al) and Niobium (Nb) become superconductors
  - At low temperatures, an attractive force appears between electrons
  - When this force gets sufficiently strong compared to thermal vibrations, electrons bind together into “Cooper pairs” with spin 1 and charge  $2q$
  - Cooper pairs form a macroscopic quantum state enabling charge to move without scattering or loss, resulting in superconductivity
- Superconductivity allows for
  - extremely low-loss RF transmission lines
  - Construction of nonlinear inductors using a Josephson junction

# At Low Temperatures Introduce Superconducting Materials such as a Josephson Tunnel Junction



Circuit Symbols



Graphic: Clarke & Wilhelm

- Two superconductors separated by a thin insulating layer
- Wave functions for superconducting Cooper pairs decay exponentially in the insulating layer
- If the layer is thin enough to allow appreciable tunneling, then phases are no longer independent but are related to each other through the size of the **tunneling current**

# Josephson Junction as a Nonlinear Inductor

$$\varphi = \varphi_2 - \varphi_1$$

$$I = I_c \sin \varphi$$

$$V = \frac{\Phi_0}{2\pi} \frac{d\varphi}{dt}, \quad \Phi_0 = \frac{h}{2q} \text{ is the flux quantum}$$

$$\frac{dI}{dt} = I_c \cos \varphi \frac{d\varphi}{dt}$$

$$= I_c \cos \varphi \frac{2\pi V}{\Phi_0}$$

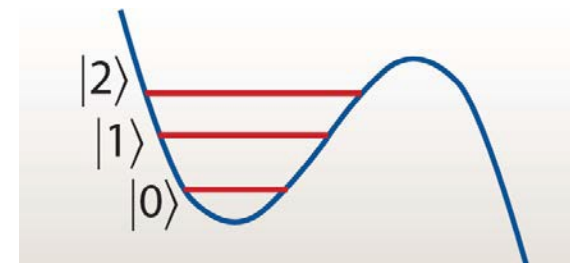
⇒

$$V = \frac{\Phi_0}{2\pi I_c \cos \varphi} \frac{dI}{dt}$$

$$= \frac{\Phi_0}{2\pi I_c \sqrt{1 - \sin^2 \varphi}} \frac{dI}{dt}$$

$$= \frac{\Phi_0}{2\pi I_c \sqrt{1 - (I/I_c)^2}} \frac{dI}{dt} = L_{\text{eff}}(I) \frac{dI}{dt}$$

- Effective inductance depends on the current
- Looks like a non-linear inductor: origin of *anharmonicity*: spacing between energy levels is not the same



- Enables the individual addressing of a single pair of states
- This is in contrast for a linear circuit where all states are equally spaced

# Various Designs for the Non-Linear Elements

- Important to know the frequencies that are driving each of the qubits
- Fine tune performance properties of the interactions between qubits
- One can choose either a fixed frequency transmon or a flux tunable transmon to address each of the energy levels
- The IBM quantum computing hardware designers selected the fixed frequency option
- Other designs (such a Rigetti's gate based quantum computing) hardware platform use a flux tunable transmon

# Fixed and Tunable Transmon Designs

## - Advantages -

### • Fixed Frequency Transmon

- Stability (remains calibrated for hours)
- No flux noise → high coherence

### • Flux Tunable Transmon

- Flexibility for faster and/or simpler 2 qubit gates
- Relaxed junction fabrication that implies avoidance of frequency collisions

# Fixed and Tunable Transmon Designs

## - Disadvantages -

### • Fixed Frequency Transmon

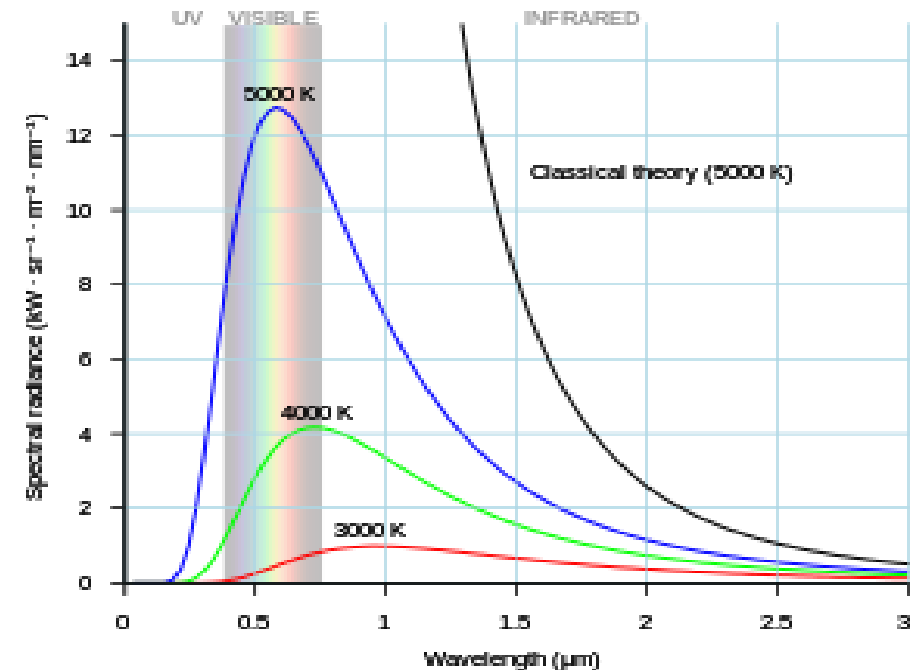
- Restricted gates requiring all microwave electronics
- Frequency collisions

### • Flux Tunable Transmon

- Flux noise leads to lower coherence
- Flux sensitivity characterized by unstable calibrations

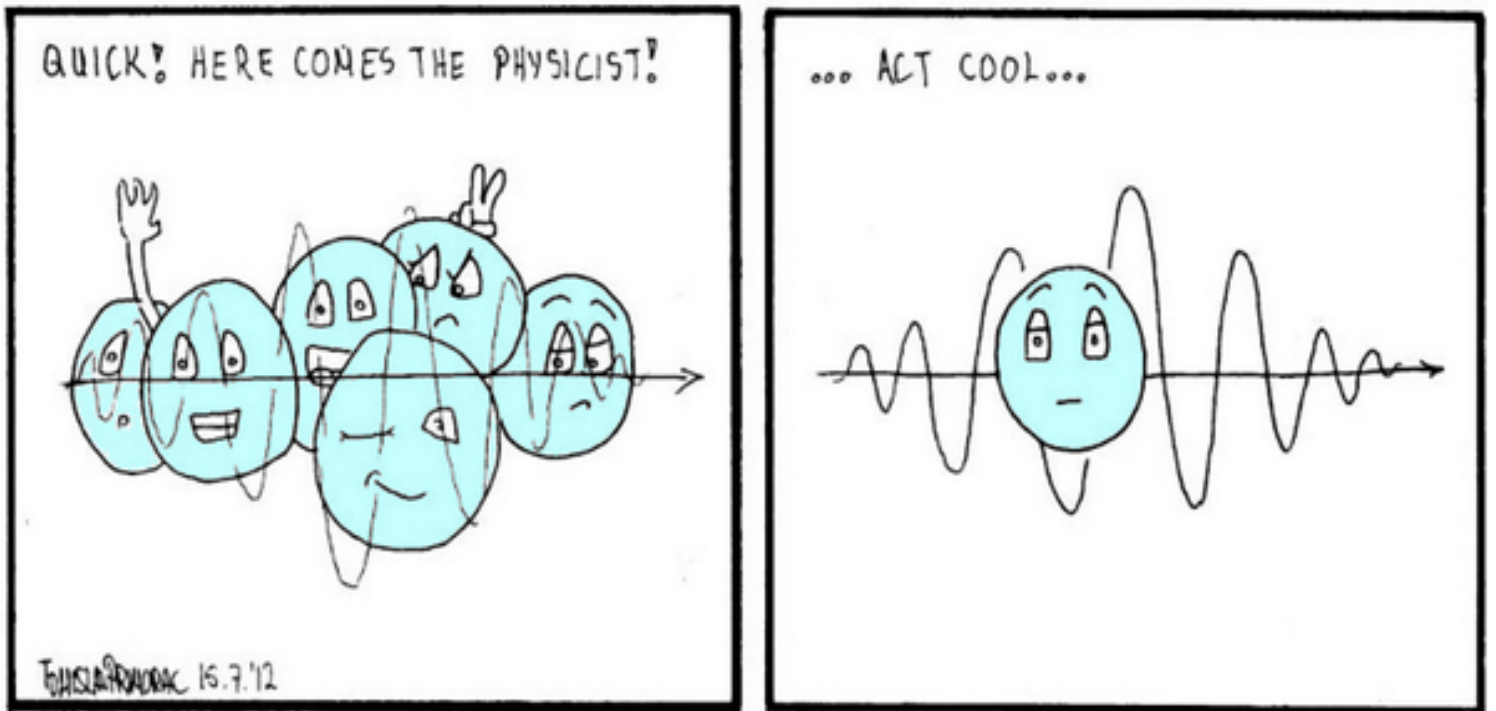
# LC Electrical Properties at Low Temperatures

- Electrical circuits operate at RF rather than optical frequencies
- Physics of thermodynamics says that any physical mass at finite temperature will emit electromagnetic radiation that depends on its temperature (Black body radiation)
- Want to design the system to be as quiescent as possible from a thermal radiation perspective – that translates into building system at low temperatures



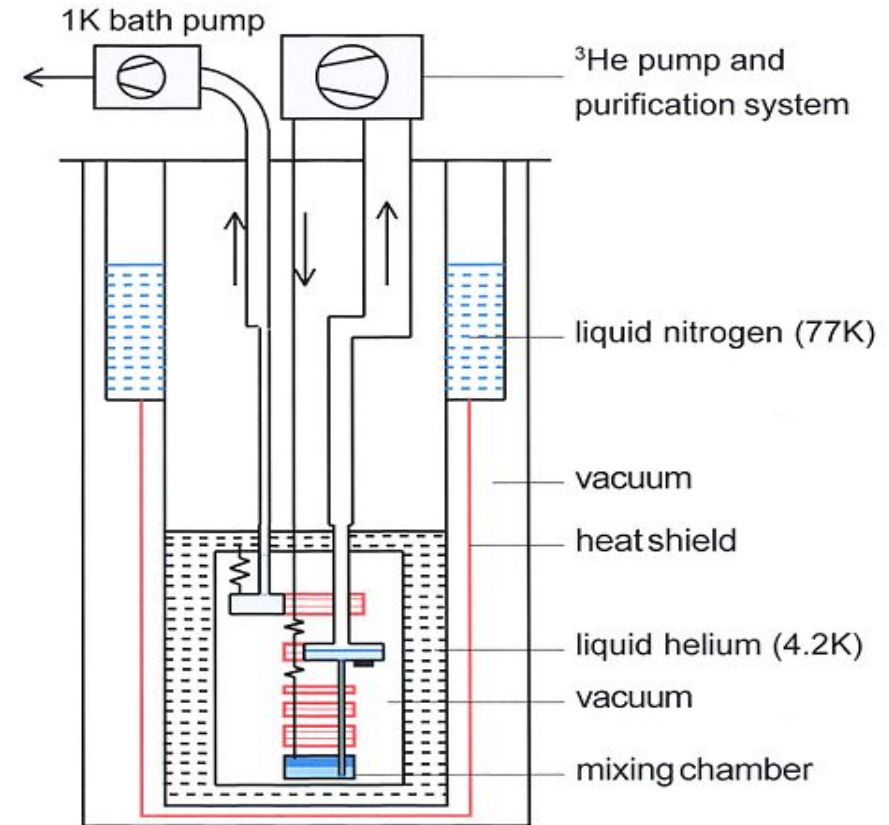
# Low Temperature Operational Requirement

- Want the energy difference between qubit states to be large compared to thermal radiation
- Highest frequency for widespread, economical design of instrumentation is  $\sim 6$  GHz
- Using equation  $kT = h\nu$  frequency of 6 GHz corresponds to approximately a temperature of 0.29K
- **Therefore the operating temperature of a QC superconducting transmon must be much less than 0.3K!**
- **100x colder than outer space (4 degrees Kelvin)**



# The IBM Superconducting Transmon Design\*

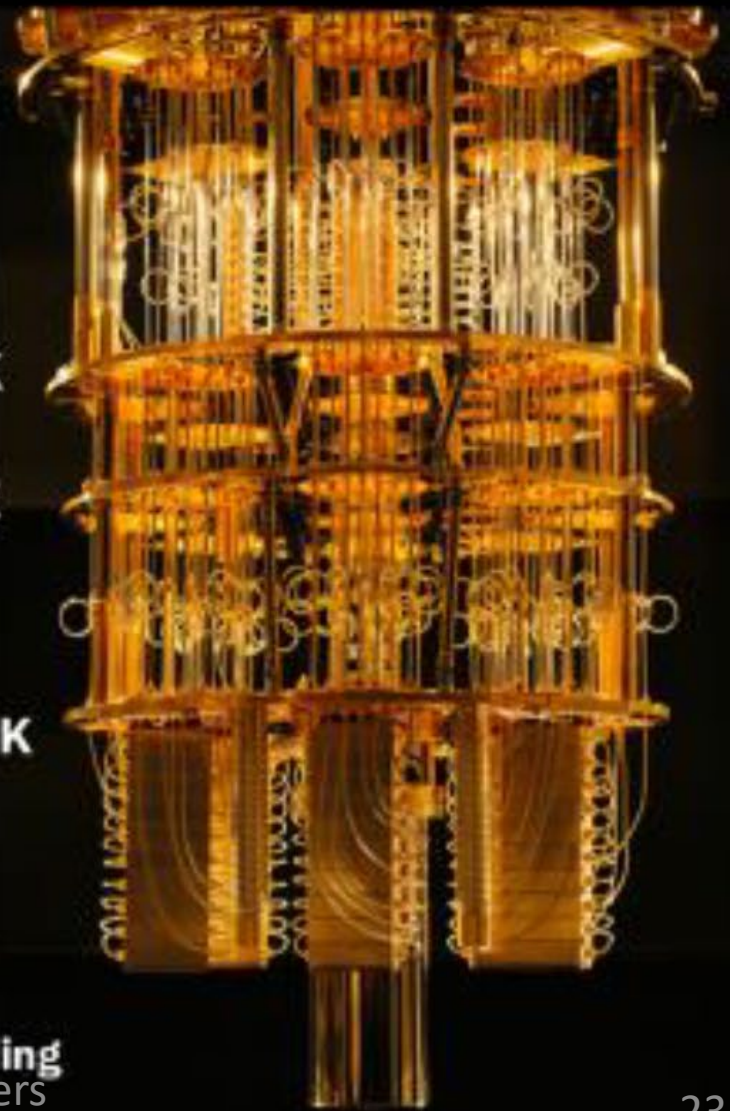
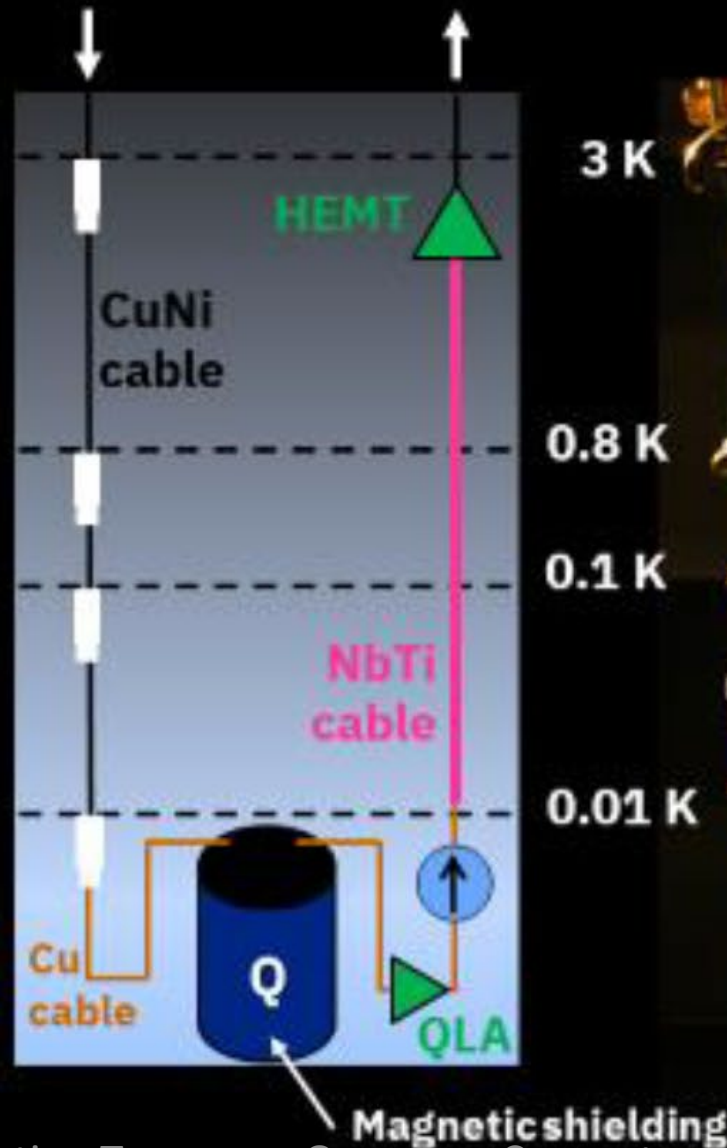
- IBM Q systems operate at a temperature of about 15 mK
- This low temperature is achieved by using dilution refrigerators



\* Image from [http://www.wikiwand.com/en/Dilution refrigerator](http://www.wikiwand.com/en/Dilution%20refrigerator)

# Getting signals to the qubits and back

- Input lines:
  - CuNi cables (low thermal conductivity, moderate electrical conductivity)
  - Attenuators at each stage
- Output lines:
  - QLA (quantum-limited amplifier)
  - Isolator (like a diode for GHz signals)
  - NbTi cable (low thermal conductivity, high electrical conductivity)
  - HEMT amplifier



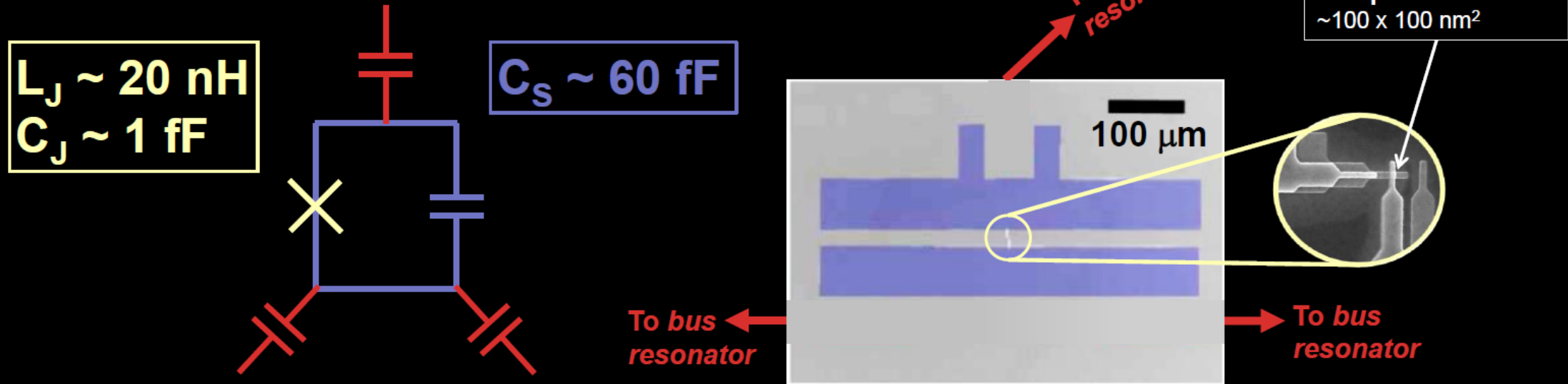
# Low Temperature Experimental Apparatus IBM Q Quantum Computer Cryostat



3 November 2020  
5 November 2020

Superconducting Transmon Quantum Computers  
Patrick Dreher

# IBM qubits: single-junction transmons



Patterned superconducting metal (**niobium + aluminum**) on silicon

– Total capacitance dominated by **shunting capacitance  $C_S$**

Interactions mediated by **capacitively coupled co-planar waveguide resonators**

– *Bus resonators* provide controlled coupling to adjacent qubits

– *Readout resonators* couple to outside world; resonant frequency indicates qubit state

# CIRCUIT QUANTUM ELECTRODYNAMICS (cQED)

- Theory: Blais et al., Phys. Rev. A **69**, 062320 (2004)

- Superconducting transmission line “cavity”

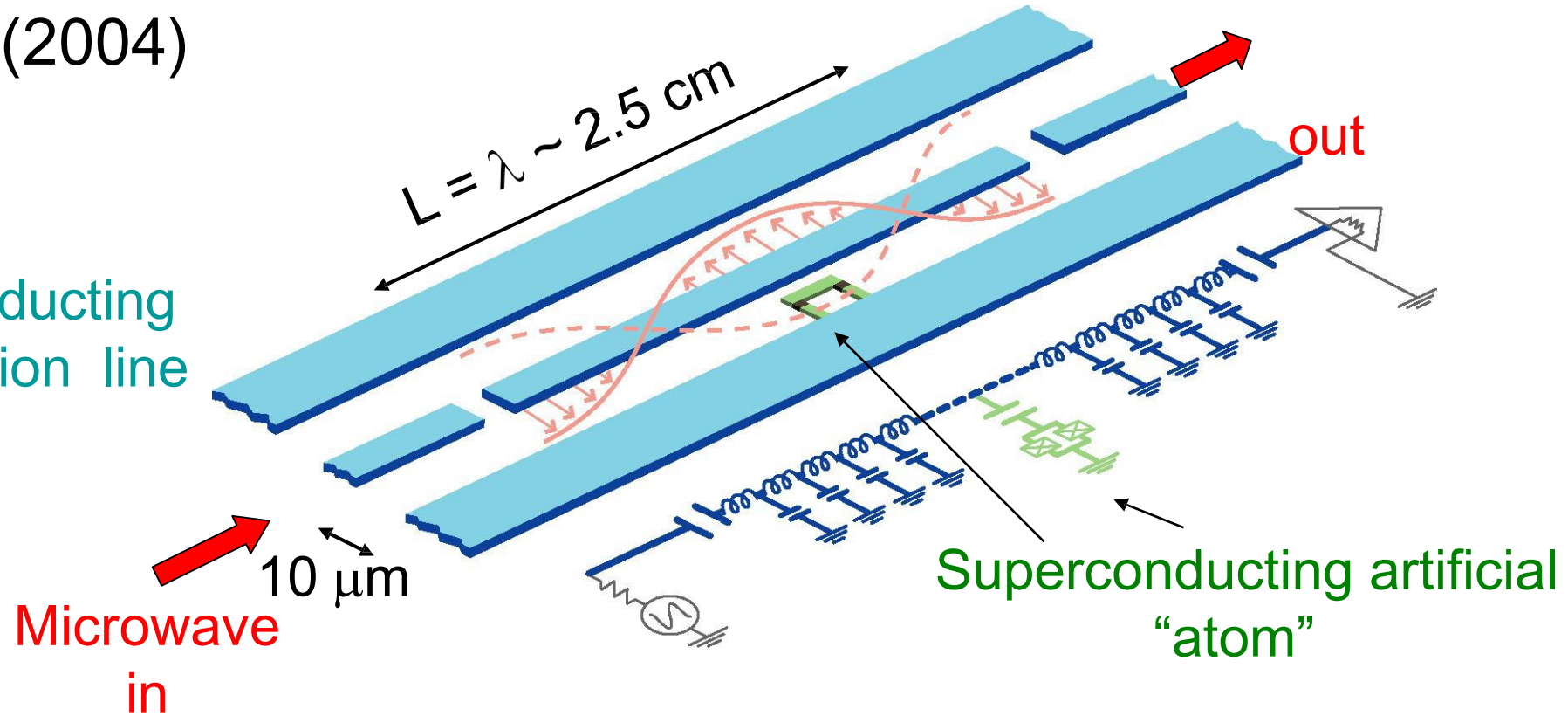
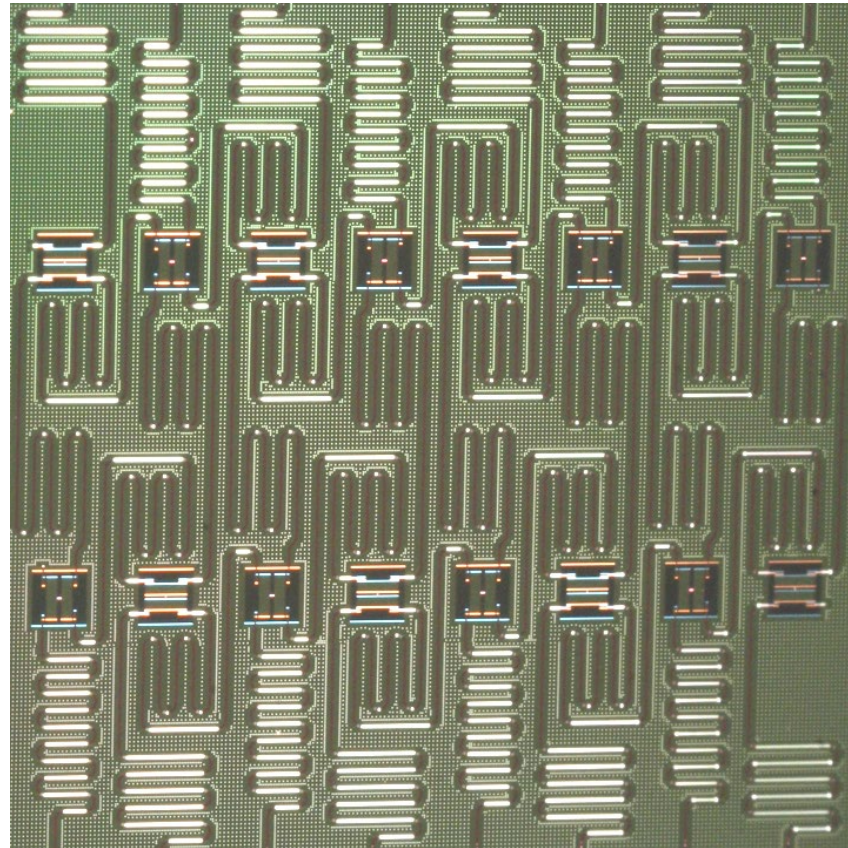


Figure from Introduction to Superconducting Qubits and Quantum Experience Hanhee Paik (2016)

3 November 2020

5 November 2020

# Superconducting Qubits on a Substrate

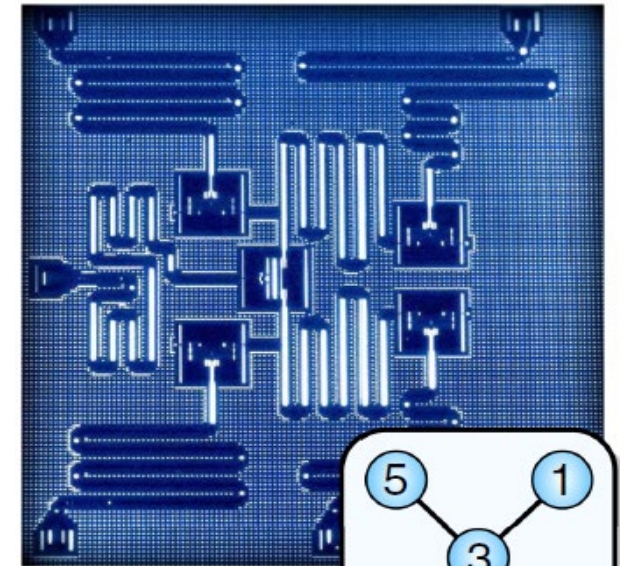
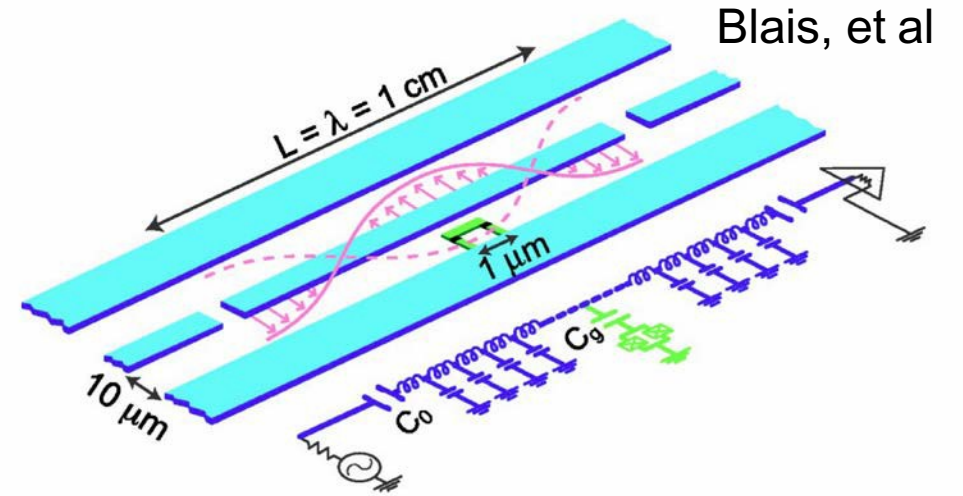


3 November 2020  
5 November 2020

Superconducting Transmon Quantum Computers  
Patrick Dreher

# Transmon Design With Example IBM Chip Layout

- Co-planar microstrip resonator formed by gaps in center conductor
- Important to properly choose resonator frequency with respect to transmon frequency
- Control is achieved by injecting an RF signal from one end
- Readout is achieved by looking at either the transmitted or reflected signal



# Working With A Hardware Platform Based on Superconducting Transmon Qubits

3 November 2020  
5 November 2020

Superconducting Transmon Quantum Computers  
Patrick Dreher

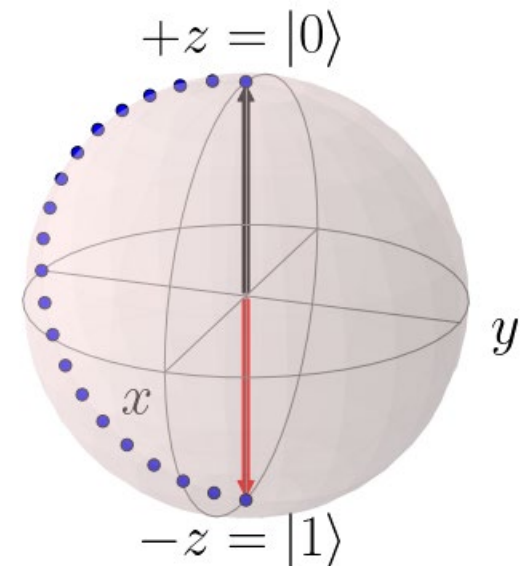
# Two State Quantum Mechanical Systems in a Superconducting Transmon Hardware Platform

3 November 2020  
5 November 2020

Superconducting Transmon Quantum Computers  
Patrick Dreher

# Importance of Understanding the Device Characteristics of Qubits

- An essential aspect for using superconducting transmon qubits is to
  - Understand their specs through their frequency characteristics and properties
  - Manually control and manipulate qubit frequencies in order to
    - Design custom gates
    - Apply noise reduction methods to extend qubit coherence lifetimes
- Need to be able to measure the frequency and the amplitude needed to achieve a  $\pi$  rotation from  $|0\rangle$  to  $|1\rangle$
- This information is essential to perform measurement characteristics of the qubit, pulse shaping and gate customization



# Goal for the Studying the Two State Quantum Mechanics Calculation

- In order to measure these quantities need to perform some calculations viewing the qubit as a two state quantum mechanical system
- Calculate the energy difference between the two states
- Solution indicates that the system will oscillate between the two states at the frequency corresponding to the energy difference
- From this observation can measure the  $\pi$ -pulse amplitude needed to transition the qubit between state  $|0\rangle$  and  $|1\rangle$  (calibrated amplitude)

# Schrodinger Equation

$$i\hbar\partial_t |\psi\rangle = H |\psi\rangle, \quad \partial_t \equiv \frac{\partial}{\partial t}$$

- $H$  is an expression for the total energy of the system (kinetic + potential) and is called the *Hamiltonian*
- For two orthogonal states:  
$$i\hbar\partial_t |1\rangle = H_0 |1\rangle = E_1 |1\rangle$$
$$i\hbar\partial_t |2\rangle = H_0 |2\rangle = E_2 |2\rangle$$
- What if we introduce a perturbation that weakly couples states 1 & 2?

$$i\hbar\partial_t |1\rangle = H_0 |1\rangle + V_{12} |2\rangle$$

$$i\hbar\partial_t |2\rangle = H_0 |2\rangle + V_{21} |1\rangle$$

# Schrodinger Equation for 2x2 coupled system

$$i\hbar\partial_t |1\rangle = H_0 |1\rangle + V_{12} |2\rangle$$

$$i\hbar\partial_t |2\rangle = H_0 |2\rangle + V_{21} |1\rangle$$

- This can be written

$$i\hbar\partial_t \begin{bmatrix} |1\rangle \\ |2\rangle \end{bmatrix} = \begin{bmatrix} E_1 & 0 \\ 0 & E_2 \end{bmatrix} \begin{bmatrix} |1\rangle \\ |2\rangle \end{bmatrix} + \begin{bmatrix} 0 & V_{12} \\ V_{21} & 0 \end{bmatrix} \begin{bmatrix} |1\rangle \\ |2\rangle \end{bmatrix} = H \begin{bmatrix} |1\rangle \\ |2\rangle \end{bmatrix}$$

$$H = \frac{1}{2}(E_1 + E_2)\sigma_0 + \frac{1}{2}(E_1 - E_2)\sigma_z + V\sigma_x, \text{ assuming } V_{12} = V_{21}$$

$$\sigma_0 = \begin{bmatrix} 1 & 0 \\ 0 & 1 \end{bmatrix}, \quad \sigma_z = \begin{bmatrix} 1 & 0 \\ 0 & -1 \end{bmatrix}, \quad \sigma_x = \begin{bmatrix} 0 & 1 \\ 1 & 0 \end{bmatrix}$$

# Formulations of Quantum Mechanics

- “Schrodinger Picture:” all time dependence is in the wave function or state vector
- “Heisenberg Picture:” all time dependence is in the Hamiltonian operator
- “Interaction Picture:” hybrid in which some time dependence is in both the operator and the state vector
  - Particularly useful when considering a small perturbation to a solved system: **express solution to perturbed system in terms of solutions to the unperturbed system**
- **See the Appendix for the detailed quantum mechanical calculation**

# Quantum Mechanics of Rabi Oscillations

- When a two-level system is coupled to a driving field at precisely the frequency corresponding to the energy difference between the states, the system will oscillate between the two states at the Rabi frequency

$$|\psi\rangle = c_g(t)|0\rangle + c_e(t)|1\rangle$$

- Initial conditions

$$c_g(0) = 1$$

$$c_e(0) = 0$$

$$P_g(t) = |c_g(t)|^2 = \frac{1}{2}(1 + \cos \Omega_R t)$$

$$P_e(t) = |c_e(t)|^2 = \frac{1}{2}(1 - \cos \Omega_R t)$$

$$\Omega_R = \frac{2}{\hbar} \langle 1 | H_I | 0 \rangle$$

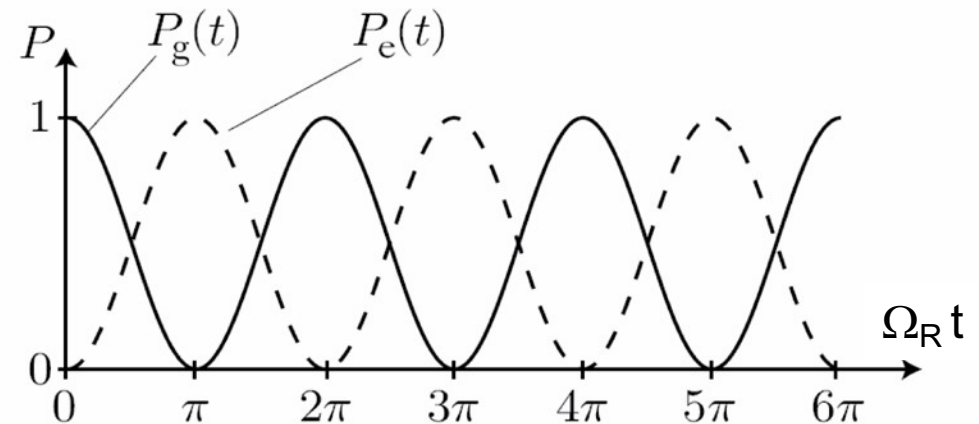


Figure 51: Time evolution of the probability  $P_g(t)$  and  $P_e(t)$  to find the atom in the ground (solid) and excited (dashed) state, respectively. [from D.A. Steck *Quantum and Atom Optics*]

# Example: Creating Gates with Rabi Oscillations

# Creating Rotations: Rabi Oscillations

- Suppose a time-varying field is applied along the x direction

$$V(t) = \hbar\Omega_R \cos(\omega_d t - \gamma),$$

- The Hamiltonian becomes

$$\mathcal{H} = -\frac{\hbar\omega_0}{2}\sigma_z + \hbar\Omega_R \cos(\omega_d t - \gamma)\sigma_x.$$

- Move to a frame rotating at  $\phi = -\omega_0 t$ ,
- Note that rotating a state vector by  $\phi$  is equivalent to rotating the coordinates by  $-\phi$ , so the state vector in the rotation frame is

$$|\psi(t)\rangle_r = U_z^\dagger(\phi) |\psi(t)\rangle. \quad U_z^\dagger(-\omega_0 t) = U_z(\omega_0 t) = e^{-i\frac{\omega_0 t}{2}\sigma_z}.$$

# Hamiltonian in the Rotating Frame

$$\begin{aligned}i\hbar\partial_t |\psi\rangle_r &= i\hbar\partial_t \left( U_z^\dagger |\psi\rangle \right) \\&= i\hbar\dot{U}_z^\dagger |\psi\rangle + U_z^\dagger (i\hbar\partial_t |\psi\rangle) \\&= i\hbar\dot{U}_z^\dagger U_z U_z^\dagger |\psi\rangle + U_z^\dagger \mathcal{H} |\psi\rangle \\&= i\hbar\dot{U}_z^\dagger U_z |\psi\rangle_r + U_z^\dagger \mathcal{H} U_z U_z^\dagger |\psi\rangle \\&= i\hbar\dot{U}_z^\dagger U_z |\psi\rangle_r + U_z^\dagger \mathcal{H} U_z |\psi\rangle_r \\&= \mathcal{H}_r |\psi\rangle_r,\end{aligned}$$

$$\mathcal{H}_r = i\hbar\dot{U}_z^\dagger U_z + U_z^\dagger \mathcal{H} U_z.$$

$$i\hbar\dot{U}_z^\dagger U_z = i\hbar\left(-i\frac{\omega_0}{2}\sigma_z\right)U_z^\dagger U_z = +\frac{\hbar\omega_0}{2}\sigma_z.$$

$$U_z^\dagger(-\omega_0 t)\sigma_z U_z(-\omega_0 t) = \sigma_z,$$

$$U_z^\dagger(-\omega_0 t)\sigma_x U_z(-\omega_0 t) = \begin{bmatrix} 0 & e^{-i\omega_0 t} \\ e^{i\omega_0 t} & 0 \end{bmatrix}.$$

# Rotating Wave Approximation

- Putting the pieces together:

$$\mathcal{H}_r = +\frac{\hbar\omega_0}{2}\sigma_z - \frac{\hbar\omega_0}{2}\sigma_z + \hbar\Omega_R \cos(\omega_d t - \gamma) \begin{bmatrix} 0 & e^{-i\omega_0 t} \\ e^{i\omega_0 t} & 0 \end{bmatrix}$$

$$= \frac{\hbar\Omega_R}{2} \begin{bmatrix} 0 & e^{i(\omega_d - \omega_0)t - i\gamma} + e^{-i(\omega_d + \omega_0)t + i\gamma} \\ e^{i(\omega_d + \omega_0)t - i\gamma} + e^{-i(\omega_d - \omega_0)t + i\gamma} & 0 \end{bmatrix}$$

tend to average out: *Rotating Wave Approximation*

$$\mathcal{H}_r = \frac{\hbar\Omega_R}{2} \begin{bmatrix} 0 & e^{i(\Delta t - \gamma)} \\ e^{-i(\Delta t - \gamma)} & 0 \end{bmatrix} \quad \Delta = \omega_d - \omega_0$$

# Time Evolution of State Vector in Rotating Frame

- If the drive frequency matches the qubit frequency,  $\Delta = 0$ .

$$\begin{aligned}\mathcal{H}_r &= \frac{\hbar\Omega_R}{2} \begin{bmatrix} 0 & e^{-i\gamma} \\ e^{+i\gamma} & 0 \end{bmatrix} \\ &= \frac{\hbar\Omega_R}{2} (\cos(\gamma)\sigma_x + \sin(\gamma)\sigma_y) \\ &= \frac{\hbar\Omega_R}{2} \hat{\mathbf{n}} \cdot \boldsymbol{\sigma},\end{aligned}$$

$$\hat{\mathbf{n}} = \hat{\mathbf{x}} \cos \gamma + \hat{\mathbf{y}} \sin \gamma. \quad |\psi(t)\rangle_r = e^{-i\mathcal{H}_r t/\hbar} |\psi(0)\rangle_r = e^{-i\frac{\Omega_R t}{2} \hat{\mathbf{n}} \cdot \boldsymbol{\sigma}} |\psi(0)\rangle_r$$

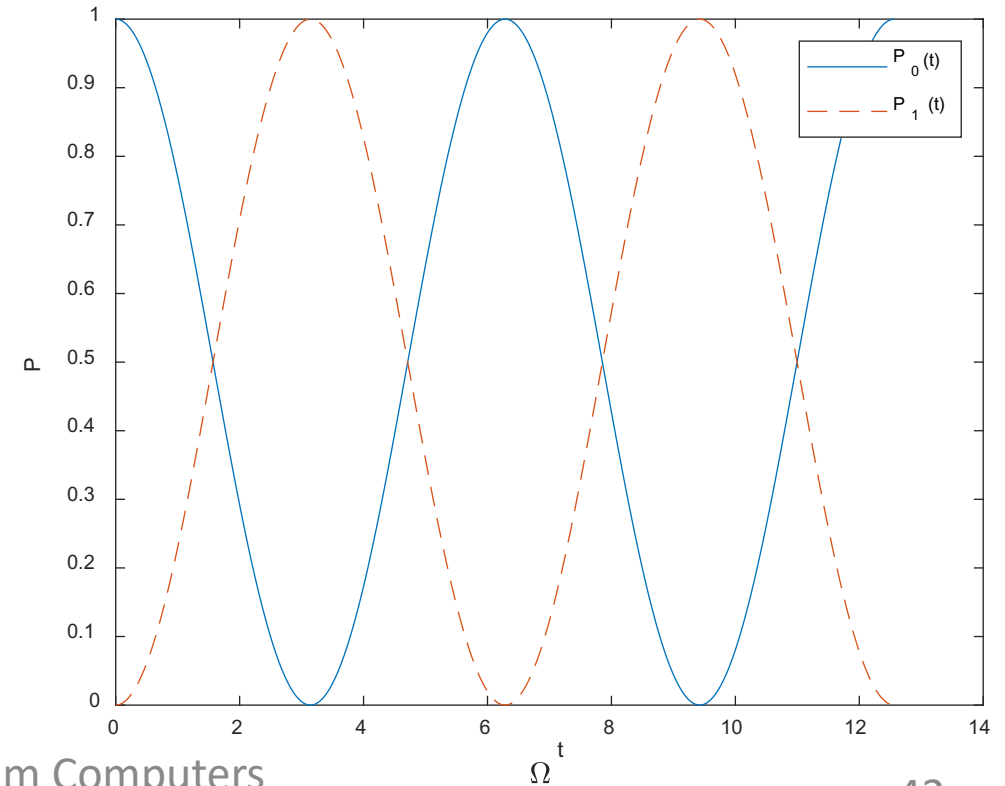
# Example: Rotation About x Axis

$$\begin{bmatrix} c_0(t) \\ c_1(t) \end{bmatrix} = \begin{bmatrix} \cos(\Omega_R t/2) & -i \sin(\Omega_R t/2) \\ -i \sin(\Omega_R t/2) & \cos(\Omega_R t/2) \end{bmatrix} \begin{bmatrix} 1 \\ 0 \end{bmatrix} = \begin{bmatrix} \cos(\Omega_R t/2) \\ -i \sin(\Omega_R t/2) \end{bmatrix}$$

$$P_0 = |c_0(t)|^2 = (\cos(\Omega_R t/2))^2 = \frac{1}{2} (1 + \cos(\Omega_R t))$$

$$P_1 = |c_1(t)|^2 = (\sin(\Omega_R t/2))^2 = \frac{1}{2} (1 - \cos(\Omega_R t))$$

- Note that the rate of rotation can be controlled by varying either the amplitude or the phase of the microwave drive signal



# Gates/Rabi Oscillations/Noise Mitigation

- Recall that when driven at resonance

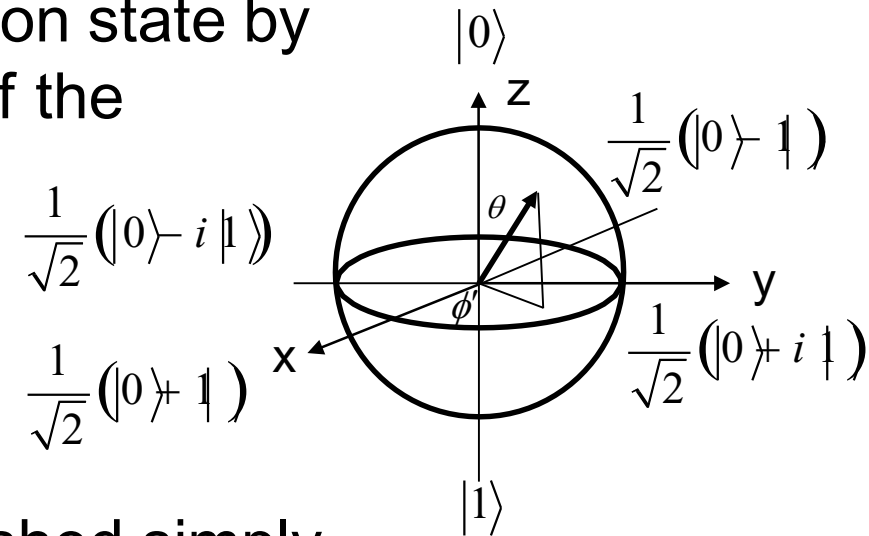
$$\begin{cases} c_1(t) = \cos(\Omega_R t / 2) \\ c_2(t) = -ie^{-i\phi} \sin(\Omega_R t / 2) \end{cases}$$

This is a key point for an important error mitigation technique: Richardson extrapolation

- “ $\pi$ -pulse”:  $\Omega_R t = \pi$  inverts the state
- “ $\pi/2$ -pulse”:  $\Omega_R t = \pi/2$  creates equal superposition of states
- Key point: you can flip a state or create a superposition state by controlling the pulse length & controlling the phase of the excitation

- X gate:  $\pi$ -pulse with  $\phi = -\pi/2$
- Y gate:  $\pi$ -pulse with  $\phi = \pi$
- Hadamard gate:  $\pi/2$ -pulse with  $\phi = -\pi/2$

- Z gate: Rotations around the z axis can be accomplished simply by resetting the phase reference of the RF drive! Result: zero time and zero error (Virtual Z Gate)



# Example: CNOT Gate

# Constructing a CNOT Gate With a Superconducting Transmon Hardware Platform

- Demonstrate can construct CNOT gate
- Consider Hamiltonian coupling two qubits where 1 and 2 refer to qubits 1 and 2 and ZZ refers to the ZZ interaction

$$H_{1,2}^{ZZ} = \frac{E_{1,2}^{ZZ}}{4} \sigma_Z^1 \otimes \sigma_Z^2$$

- This interaction term corresponds to a unitary time-evolution given by

$$U_{1,2}^{ZZ} = \exp[-iH_{1,2}^{ZZ}t]$$

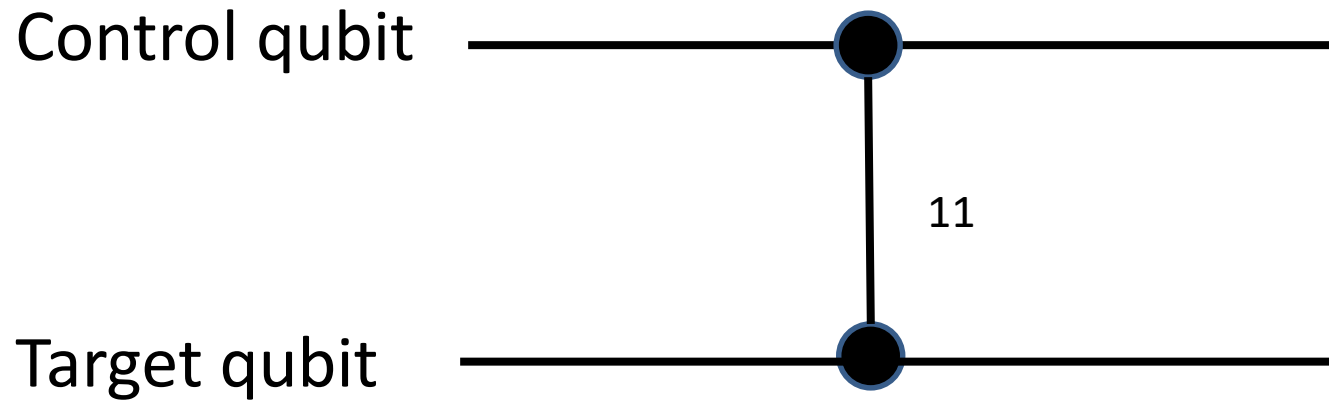
- Turn interaction on and off over a time  $t = \frac{h}{2E_{1,2}^{ZZ}}$

- Use computational basis  $|0,0\rangle$  with a corresponding vector of  $(1,0,0,0)$  to construct the unitary operation

$$U_{1,2}^{ZZ} = \exp\left[\frac{i\pi}{4}\right] \begin{bmatrix} 1 & 0 & 0 & 0 \\ 0 & -i & 0 & 0 \\ 0 & 0 & -i & 0 \\ 0 & 0 & 0 & 1 \end{bmatrix}$$

- This unitary operation can be combined with rotations around  $z$  of each qubit  $R_z^1$  ( $-\pi/2$ ) and  $R_z^2$  ( $\pi/2$ ) up to a global phase factor

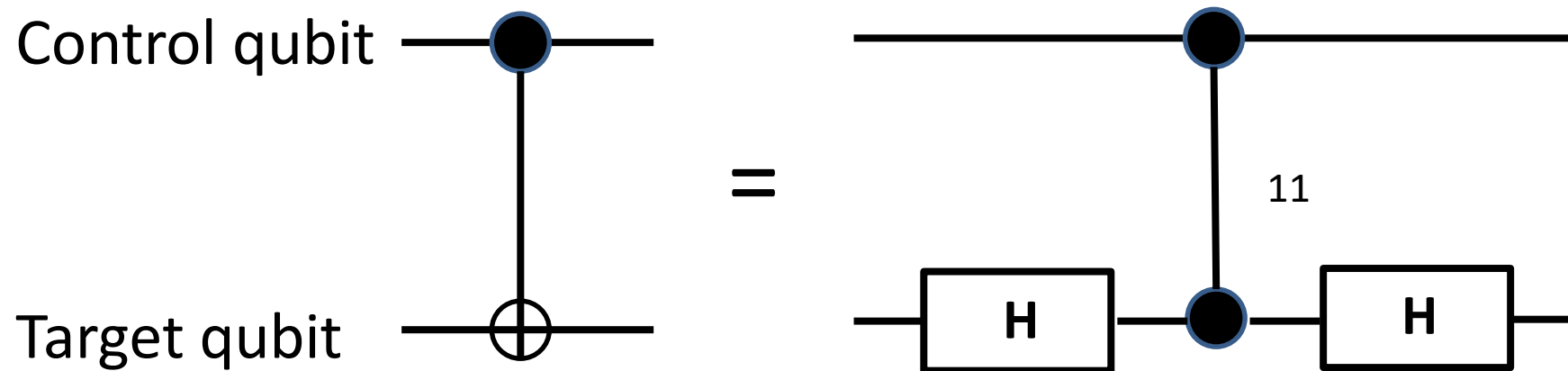
# C-Phase Gate



$$cU_{1,1} = [R_Z^i(-\pi/2) \otimes R_Z^j(-\pi/2)] U_{1,2}^{ZZ} = \exp\left[\frac{i\pi}{4}\right] \begin{bmatrix} 1 & 0 & 0 & 0 \\ 0 & 1 & 0 & 0 \\ 0 & 0 & 1 & 0 \\ 0 & 0 & 0 & -1 \end{bmatrix}$$

# CNOT Gate Relation to C-Phase Gate

- This  $cU_{11}$  c-Phase gate corresponds to a phase shift of  $\pi$  on the target qubit excited state when the control qubit is in the excited state  $|1\rangle$
- The CNOT and C-Phase gates differ by only single qubit rotations
- The CNOT gate can be constructed using the C-Phase Gate with Hadamard gates on the target qubit



# CNOT Gate Calculation

- Write the outer product representation of the combined Hadamard and c-Phase gates

$$U_{CNOT} = \exp\left(\frac{i\pi}{4}\right) \frac{1}{\sqrt{2}} \left( \begin{array}{cc|cc} 1 & 1 & 0 & 0 \\ 1 & -1 & 0 & 0 \\ \hline 0 & 0 & 1 & 1 \\ 0 & 0 & 1 & -1 \end{array} \right) \left( \begin{array}{cc|cc} 1 & 0 & 0 & 0 \\ 0 & 1 & 0 & 0 \\ \hline 0 & 0 & 1 & 0 \\ 0 & 0 & 0 & -1 \end{array} \right) \frac{1}{\sqrt{2}} \left( \begin{array}{cc|cc} 1 & 1 & 0 & 0 \\ 1 & -1 & 0 & 0 \\ \hline 0 & 0 & 1 & 1 \\ 0 & 0 & 1 & -1 \end{array} \right)$$

$$U_{CNOT} = \exp\left(\frac{i\pi}{4}\right) \left( \begin{array}{cc|cc} 1 & 0 & 0 & 0 \\ 0 & 1 & 0 & 0 \\ \hline 0 & 0 & 0 & 1 \\ 0 & 0 & 1 & 0 \end{array} \right)$$

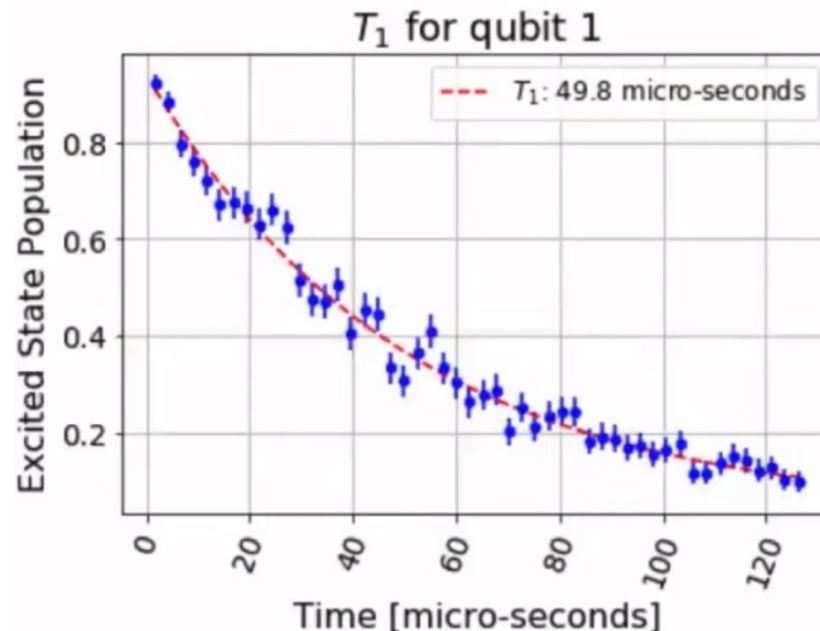
# Performance Metrics for Superconducting Transmon Hardware

3 November 2020  
5 November 2020

Superconducting Transmon Quantum Computers  
Patrick Dreher

# $T_1$ – Relaxation Time

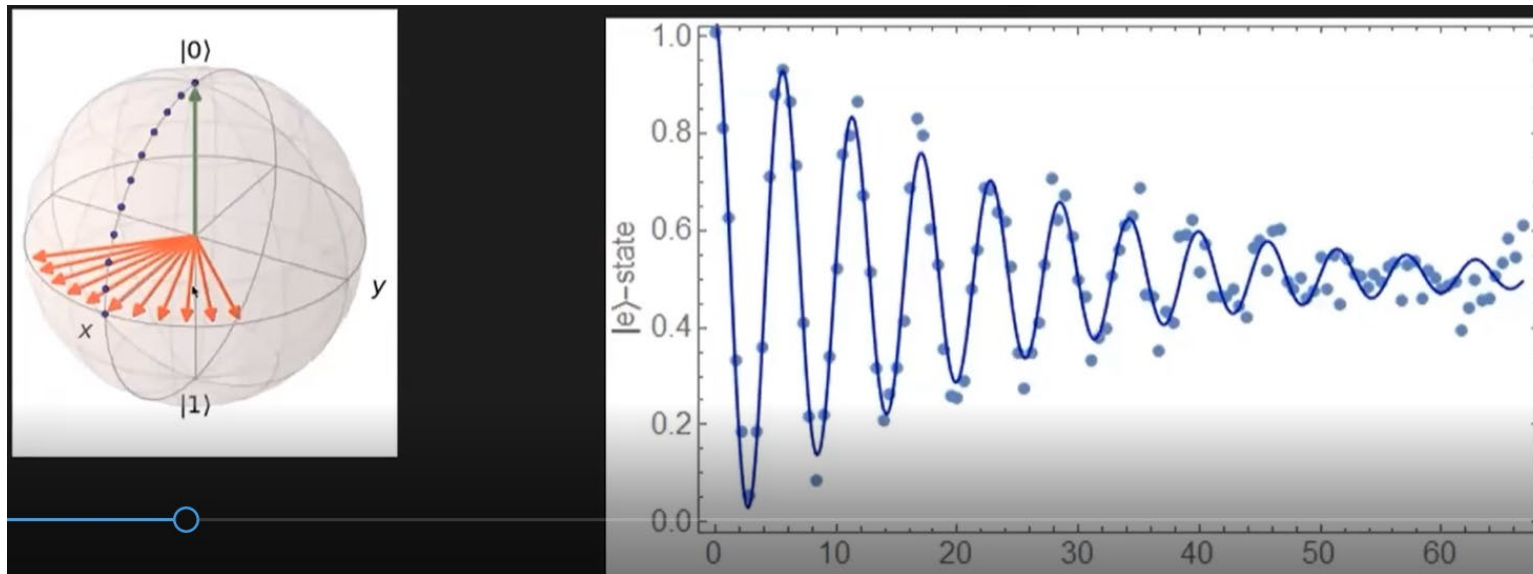
- Initialize with qubit in the ground state  $|0\rangle$
- Put the qubit into the  $|1\rangle$  state by applying an X-gate ( $\pi$ -pulse)
- Wait a specified period of time and then measure in the relaxation time of the qubit from  $|1\rangle$  state  $\rightarrow$   $|0\rangle$
- Find the relaxation rate by fitting and exponential decay curve to the data



IBM figure from Device Characteristics presentation

# Qubit De-Phasing ( $T_\phi$ )

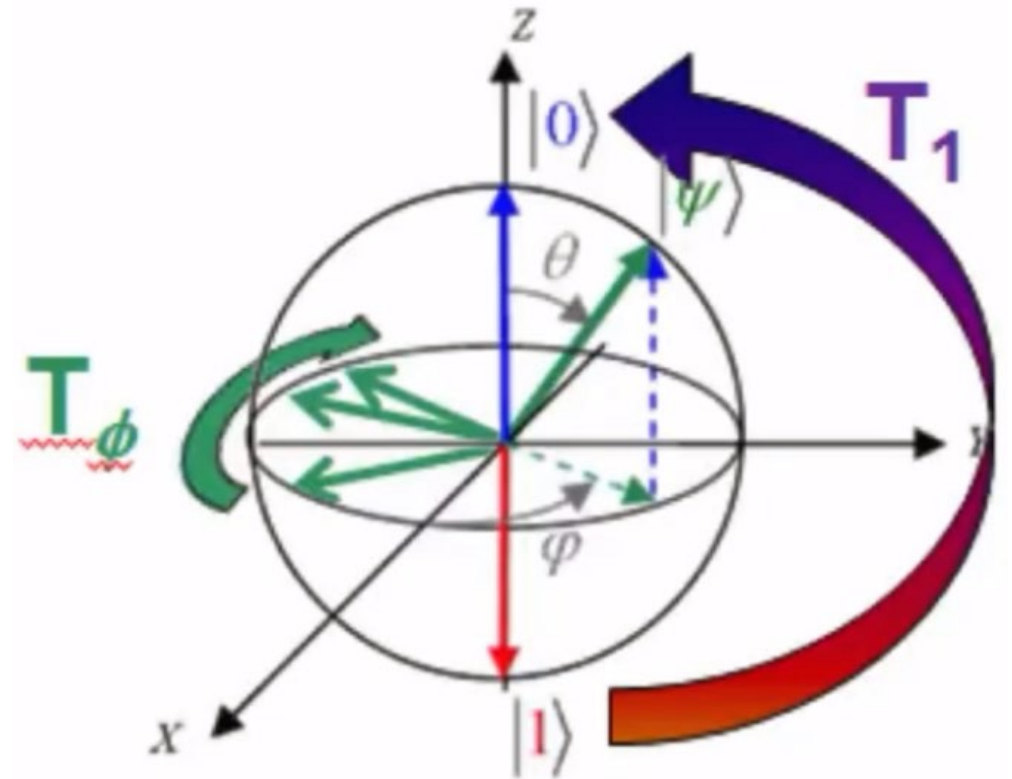
- Initialize with qubit in the ground state  $|0\rangle$
- Transform the qubit into a superposition state
- Allow the qubit state to evolve over time
- Measure the qubit state (dephasing)



# Overall Qubit Decoherence Measurements and Characteristics

- Measure a loss of quantum information due to interactions with environmental factors
- $T_1$  is a relaxation time
- $T_\phi$  is a dephasing time
- $T_2$  is the overall decoherence time

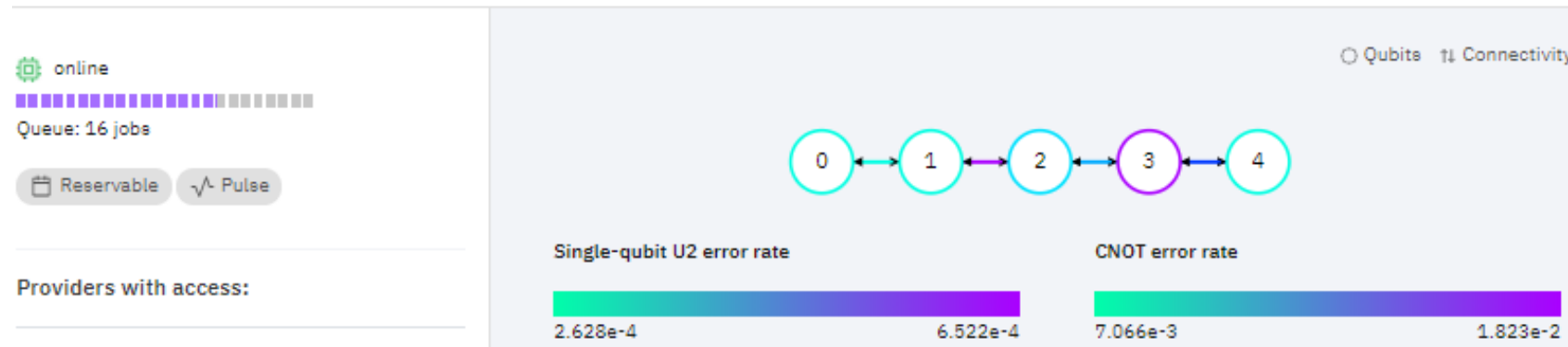
$$\frac{1}{T_2} = \frac{1}{2T_1} + \frac{1}{T_\phi}$$



IBM figure from Device Characteristics presentation

# Specification Data for an IBM Q Hardware Platform

ibmq\_rome v1.1.4



| Qubit | T1 ( $\hat{\text{A}}\mu\text{s}$ ) | T2 ( $\hat{\text{A}}\mu\text{s}$ ) | Frequency (GHz) | Readout error | Single-qubit U2 error rate | CNOT error rate                  | Date                                    |
|-------|------------------------------------|------------------------------------|-----------------|---------------|----------------------------|----------------------------------|---|
| Q0    | 58.8833343                         | 65.40557317                        | 4.968658551     | 1.12E-02      | 2.63E-04                   | cx0_1: 7.066e-3                  | Tue Oct 27 2020 03:06:12 GMT-0400 (EDT) |
| Q1    | 155.7258209                        | 59.31927948                        | 4.770375545     | 4.17E-02      | 2.69E-04                   | cx1_0: 7.066e-3, cx1_2: 1.823e-2 | Tue Oct 27 2020 03:06:12 GMT-0400 (EDT) |
| Q2    | 81.77066486                        | 98.2056677                         | 5.015085378     | 5.55E-02      | 3.38E-04                   | cx2_1: 1.823e-2, cx2_3: 1.060e-2 | Tue Oct 27 2020 03:06:12 GMT-0400 (EDT) |
| Q3    | 32.06346406                        | 25.34362315                        | 5.259407406     | 2.39E-02      | 6.52E-04                   | cx3_2: 1.060e-2, cx3_4: 1.292e-2 | Tue Oct 27 2020 03:06:12 GMT-0400 (EDT) |
| Q4    | 61.77515414                        | 120.4829221                        | 4.997495545     | 8.70E-03      | 2.85E-04                   | cx4_3: 1.292e-2                  | Tue Oct 27 2020 03:06:12 GMT-0400 (EDT) |

# Entangled Qubits

3 November 2020  
5 November 2020

Superconducting Transmon Quantum Computers  
Patrick Dreher

# Multi-Qubit Computations

- One of the advantages of quantum computing is the ability to entangle qubits
- This expands the computational power of these hardware platforms
- The process of entangling qubits is connected to
  - Understanding the operational frequency of each qubit
  - Ability to shape and customize the pulses for each calculation
  - Ability to successfully read-out the final states of the qubits

# Hamiltonian for Two Coupled Qubits

- Hamiltonian for two coupled qubits, each with an RF drive perturbation

$$H = \frac{1}{2} \hbar \omega_1 \sigma_1^z + V_1 \cos(\omega_1^{rf} t + \phi_1) \sigma_1^x + \frac{1}{2} \hbar \omega_2 \sigma_2^z + V_2 \cos(\omega_2^{rf} t + \phi_2) \sigma_2^x + \frac{1}{2} \hbar \omega_{xx} \sigma_1^x \otimes \sigma_2^x$$

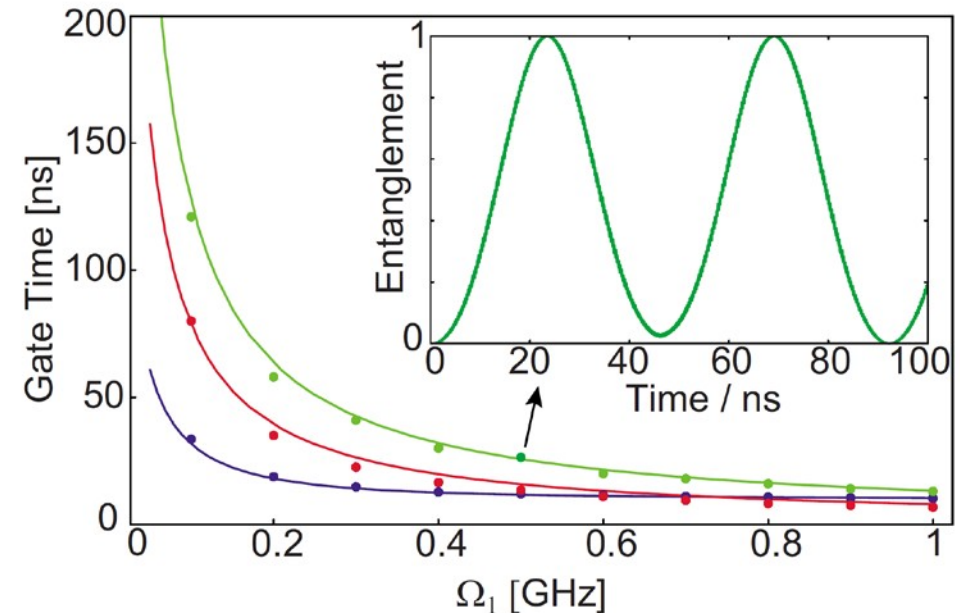
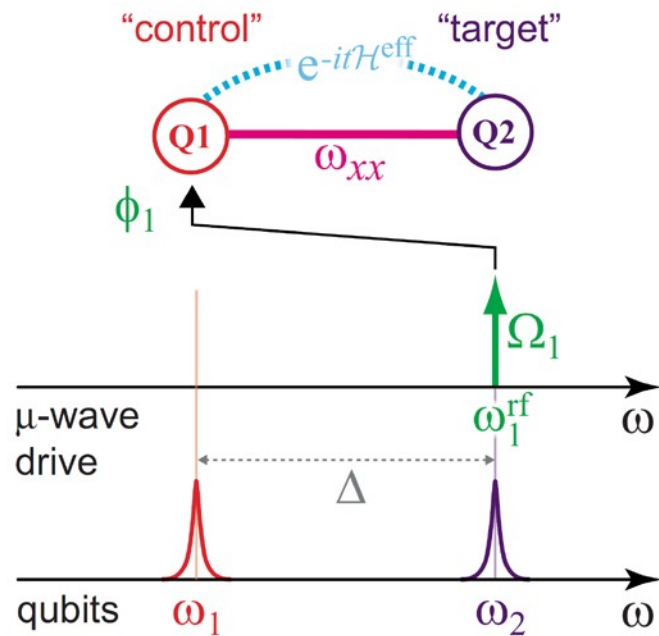
- If  $V_2=0$ , and we drive the first qubit at the resonance frequency of the second, we have the *cross-resonance condition*  $\omega_1^{rf} = \omega_2$
- After multiple transformations and making the rotating wave approximation, this can be expressed

$$H^{eff} = \frac{1}{2} \hbar \omega_{xx}^{eff} (\cos \phi_1 \sigma_1^z \otimes \sigma_2^x + \sin \phi_1 \sigma_1^x \otimes \sigma_2^y), \quad \omega_{xx}^{eff} = \frac{V_1 \omega_{xx}}{2\hbar(\omega_2 - \omega_1)}$$

- When  $\omega_{xx}^{eff} t = \pi/2$  this implements a ZX gate, and along with two single qubit gates this enables the realization of a CNOT

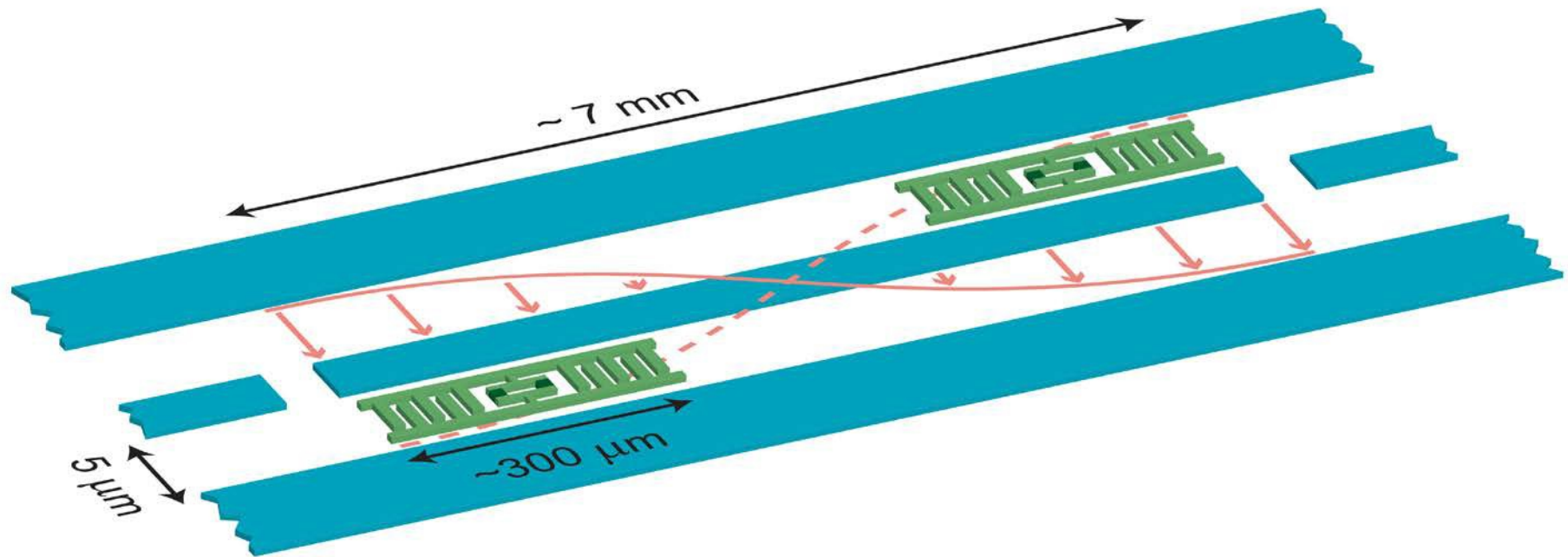
# Cross-resonant Coupling

- Frequency switches on coupling
- Amplitude controls the gate speed
- Phase determines the two-qubit gate



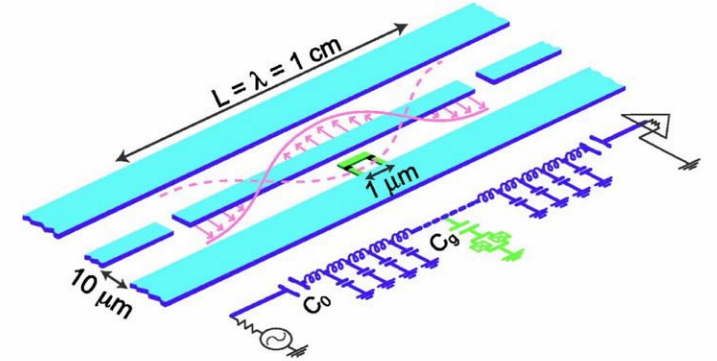
# Entangling two qubits with a quantum bus

- “Dispersive coupling”: coplanar waveguide resonator detuned from either qubit frequency



# Interactions between Qubits

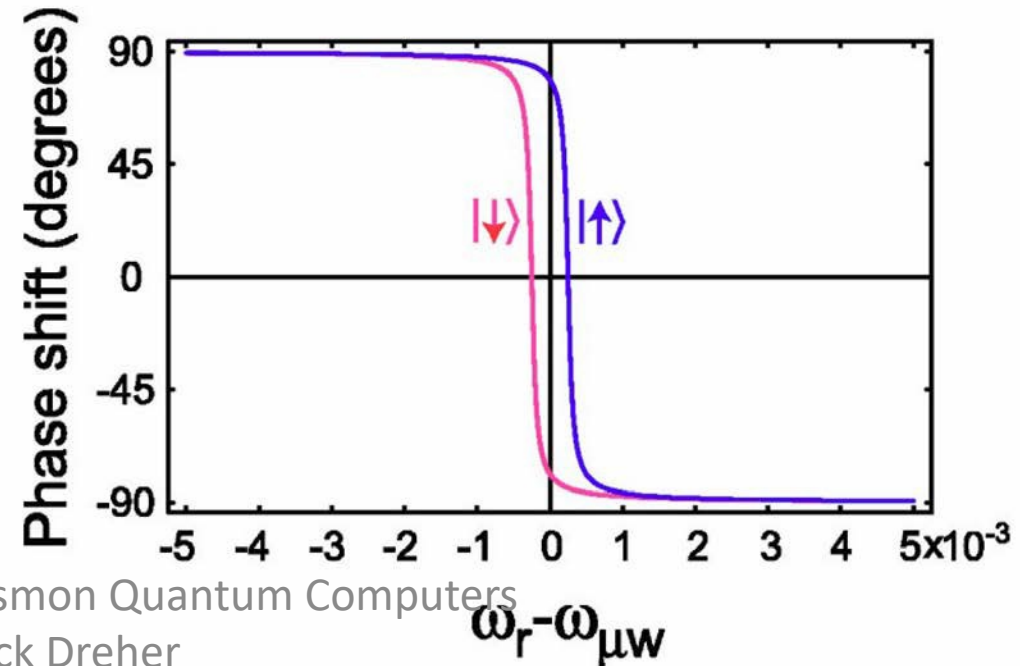
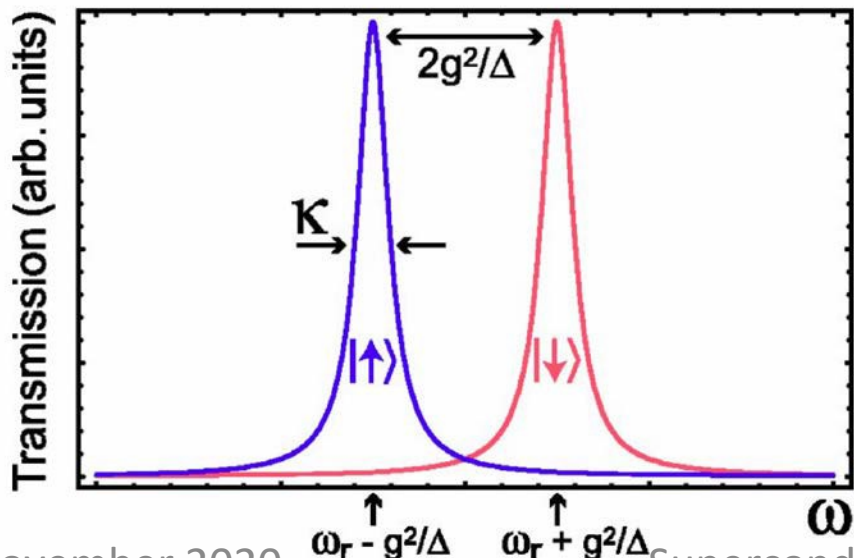
- Co-planar microstrip resonator formed by gaps in center conductor
- Important to properly choose resonator frequency with respect to transmon frequency
- Control is achieved by injecting an RF signal from one end
- Readout is achieved by looking at either the transmitted or reflected signal



Blais, et al

# Control and Read-out

- When the microstrip resonator is detuned from the transmon frequency, interaction with the transmon splits the resonator response into two modes, depending on the transmon state
- Sending in a pulse near  $\omega_r$  enables you to read-out the state either from the phase, or the amplitude
- Sending in a pulse detuned from the microstrip resonator but tuned to the qubit frequency rotates the state, but does not make a measurement (there is no information about the state in the reflected signal, the resonator is so far off resonance)



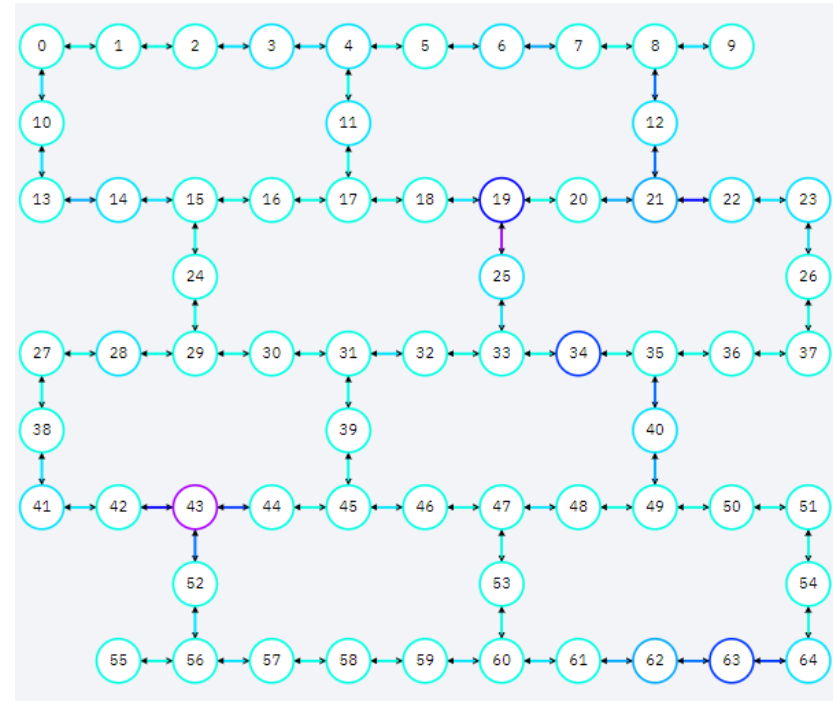
# Final Summary and Observations

3 November 2020  
5 November 2020

Superconducting Transmon Quantum Computers  
Patrick Dreher

# Development Trajectory for Superconducting Transmon Quantum Computing Hardware Platforms

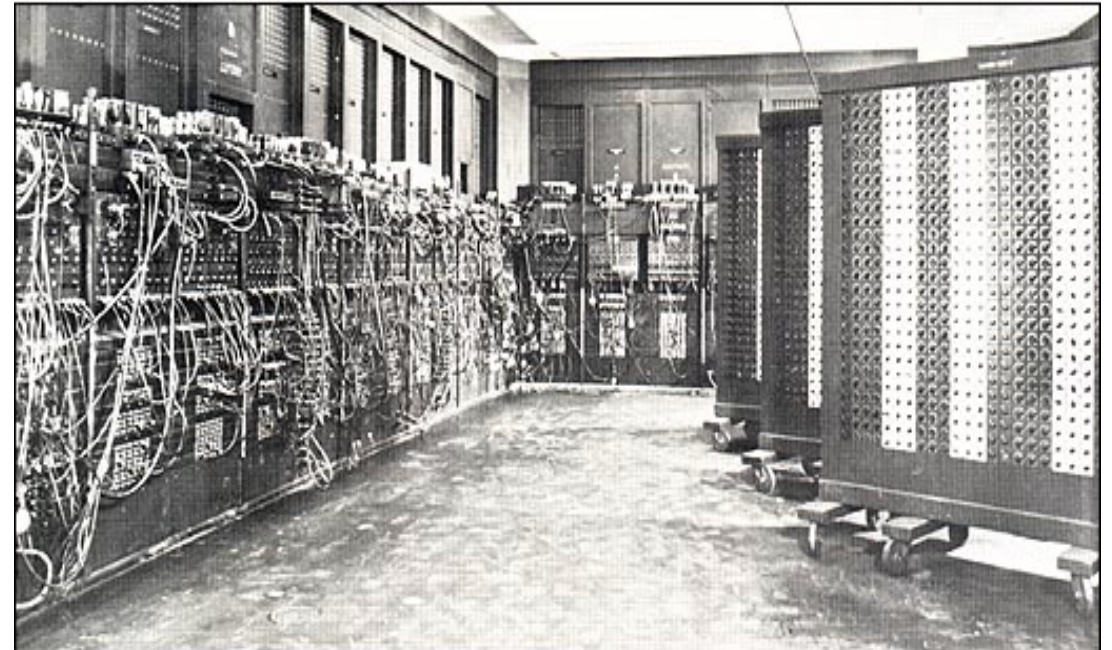
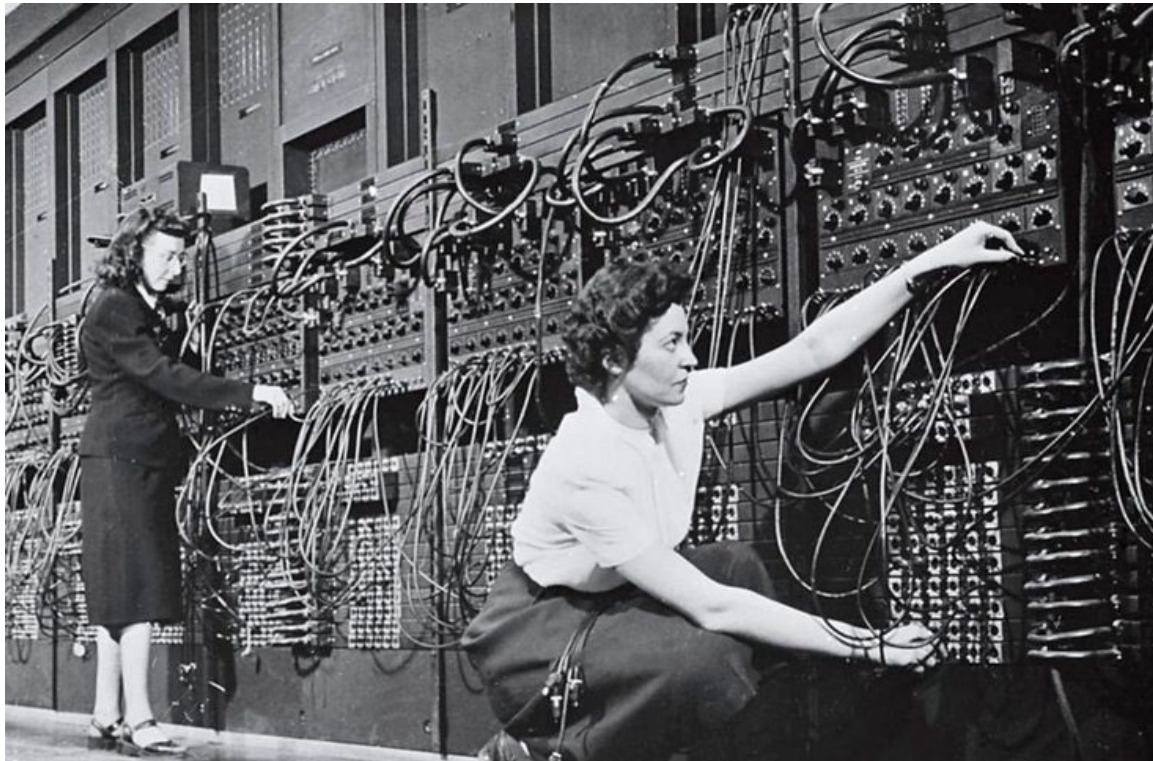
- After exploring several different designs for qubit placement on a substrate, the IBM designers have committed to expanding a “heavy hex” topology
- Tradeoffs
  - less crosstalk with fewer qubit interconnects
  - Because qubits must be adjacent for computation, it will require more SWAP gates to be inserted into the circuits
  - Optimization with “pulse control”



IBM's  
Manhattan  
QC platform  
65 qubits

# Early Digital Computing Hardware

## ENIAC Machine Room ~ 1950



Among the first assignments given to Eniac, first all-electronics digital computer, was a knotty problem in nuclear physics. It produced the answer in two hours. One hundred engineers using conventional methods would have needed a year to solve the problem

# Digital Computer Technology Seventy Years Later in 2020



Google's London data center  
for Cloud Computing

3 November 2020  
5 November 2020

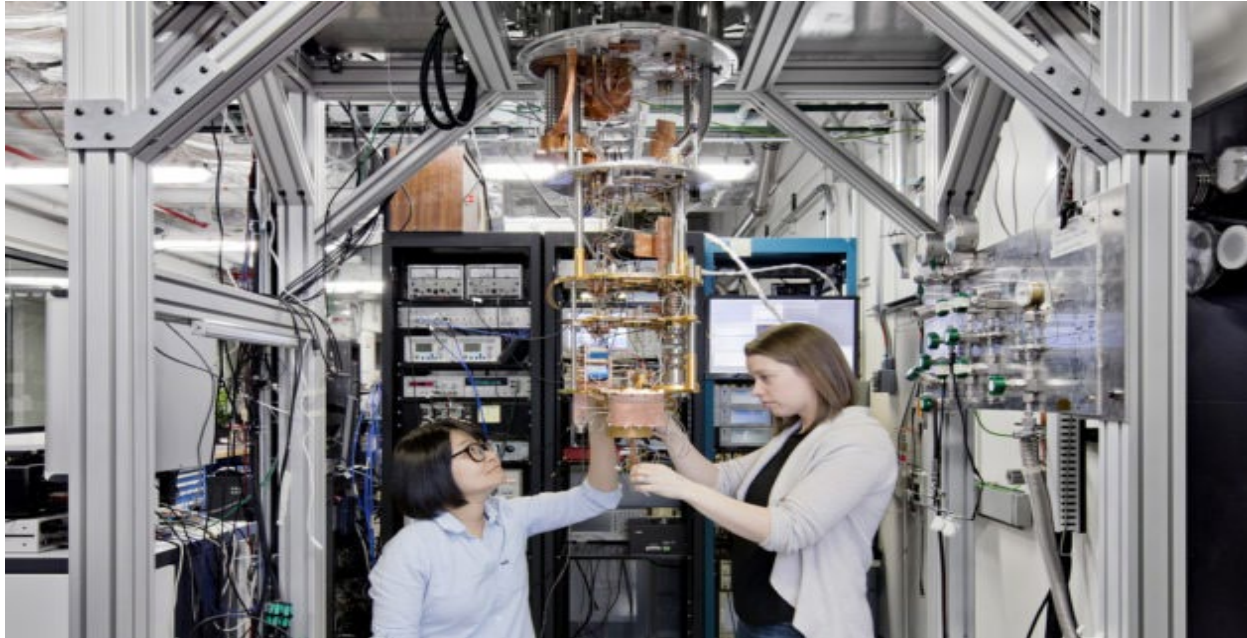


SUMMIT Supercomputer  
Oak Ridge National  
Laboratory

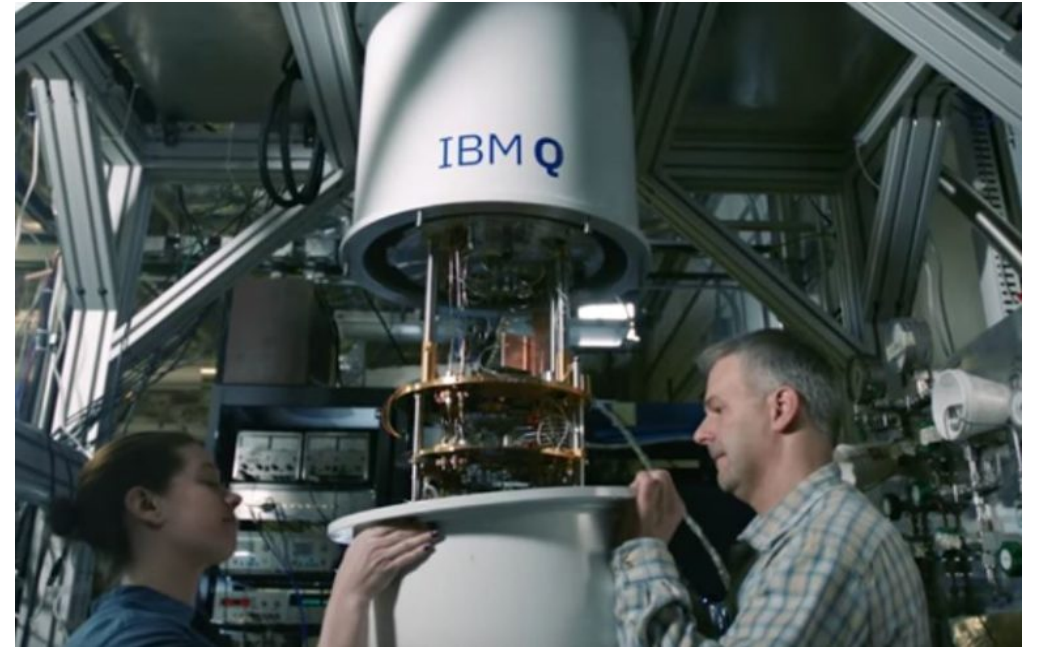
Superconducting Transmon Quantum Computers  
Patrick Dreher

# Quantum Computing Technology

## IBM Q Machine Room - 2020

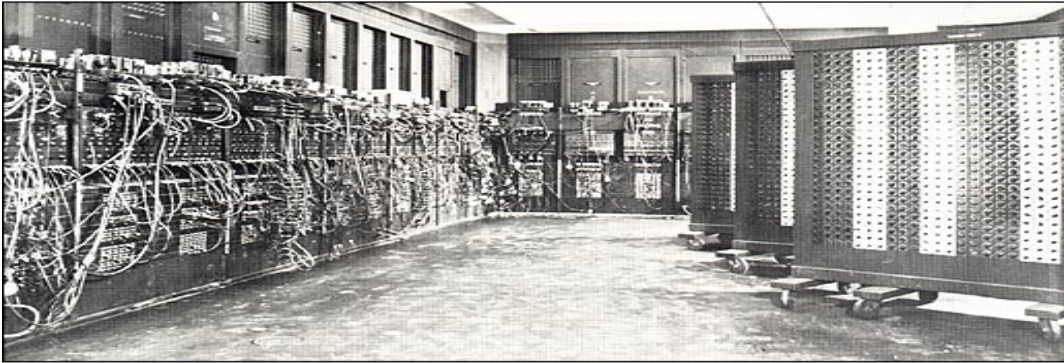


3 November 2020  
5 November 2020

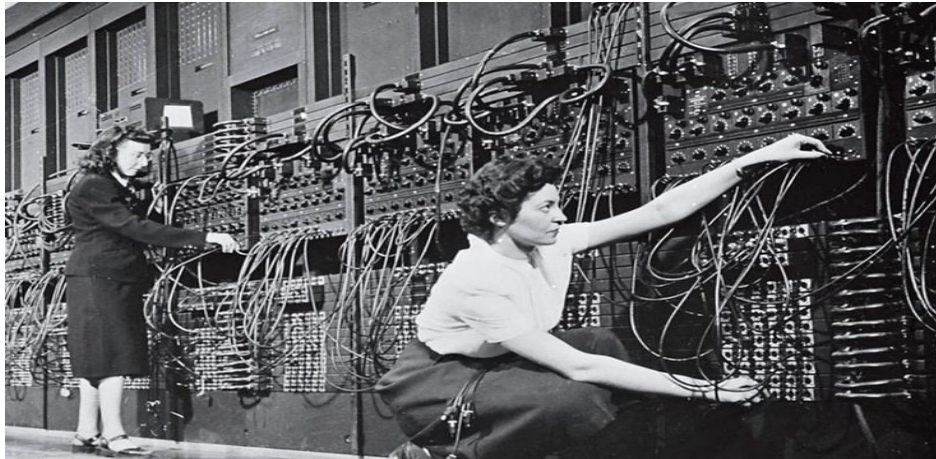


Superconducting Transmon Qubits  
Patrick Dreher

# We are in the Early Days of Quantum Computing



Among the first assignments given to Eniac, first all-electronics digital computer, was a knotty problem in nuclear physics. It produced the answer in two hours. One hundred engineers using conventional methods would have needed a year to solve the problem



Source: Anthony Annunziata, IBM

## IBM Q Quantum Computing Machine Room, 2020

3 November 2020  
5 November 2020

Superconducting Transmon Quantum Computers  
Patrick Dreher

# Quantum Computing Technology in 2090



3 November 2020  
5 November 2020

Superconducting Transmon Quantum Computers  
Patrick Dreher

# Questions

3 November 2020  
5 November 2020

Superconducting Transmon Quantum Computers  
Patrick Dreher

# Appendices

- References
- Quantum mechanical solution of the 2 level system\*

\*Some of the slides are shared as a courtesy from a lecture by Professor Stancil to the CSC591 course in 2018

# References

**From D. Stancil, Quantum Computing CSC591/ECE592, 24 Sept. 2018**

- A. Blais, et al, “Cavity quantum electrodynamics for superconducting electrical circuits: An architecture for quantum computation,” Phys. Rev. A, Vol. 9, 062320 (2004)
- J. Koch, et al, “Charge-insensitive qubit design derived from the Cooper Pair Box,” Phys. Rev. A Vol. 76, 042319 (2007).
- J. Clarke & F. Wilhelm, “Superconducting quantum bits,” Nature, Vol. 453, 19 June 2008, p. 1031.
- J.M. Chow, “Quantum Information Processing with Superconducting Qubits,” Ph.D. Dissertation, Yale Univ., 2010.
- C.T. Rigetti, “Quantum Gates for Superconducting Qubits,” Ph.D. Dissertation, Yale Univ., 2009.
- C. Rigetti and M. Devoret, “Fully microwave-tunable universal gates in superconducting qubits with linear couplings and fixed transition frequencies,” Phys. Rev. B vol. 81, 134507 (2010)
- T. Van Duzer and C.W. Turner, “Principles of Superconductive Devices and Circuits,” Elsevier, 1981.
- A. Kandala, A. Mezzacapo, K. Temme, M. Takita, M. Brink, J.M. Chow and J.M. Gambetta, “Hardware-efficient variational quantum eigensolver for small molecules and quantum magnets,” Nature, Vol. 549, p. 242 (2017).

# Reference

## A Quantum Engineer's Guide to Superconducting Qubits

Krantz, Kjaergaard, Yan, Orlando, Gustavsson, and Oliver

arXiv 1904.06560

3 November 2020  
5 November 2020

Superconduct

arXiv:1904.06560v3 [quant-ph] 9 Aug 2019

## A Quantum Engineer's Guide to Superconducting Qubits

P. Krantz<sup>1,2,†</sup>, M. Kjaergaard<sup>1</sup>, F. Yan<sup>1</sup>, T.P. Orlando<sup>1</sup>, S. Gustavsson<sup>1</sup>, and W. D. Oliver<sup>1,3,‡</sup>

<sup>1</sup>Research Laboratory of Electronics, Massachusetts Institute of Technology, Cambridge, MA 02139, USA

<sup>2</sup>Wallenberg Centre for Quantum Technology (WACQT), Chalmers University of Technology, Gothenburg, SE-41296, Sweden and

<sup>3</sup>MIT Lincoln Laboratory, 244 Wood Street, Lexington, MA 02420, USA

(Dated: 12 August 2019)

The aim of this review is to provide quantum engineers with an introductory guide to the central concepts and challenges in the rapidly accelerating field of superconducting quantum circuits. Over the past twenty years, the field has matured from a predominantly basic research endeavor to one that increasingly explores the engineering of larger-scale superconducting quantum systems. Here, we review several foundational elements – qubit design, noise properties, qubit control, and readout techniques – developed during this period, bridging fundamental concepts in circuit quantum electrodynamics (cQED) and contemporary, state-of-the-art applications in gate-model quantum computation.

### CONTENTS

|   |    |  |    |
|---|----|--|----|
| <b>I. Introduction</b>                                    | 2  | 1. Connecting $T_1$ to $S(\omega)$   | 19 |
| A. Organization of this article                           | 2  | 2. Connecting $T_2$ to $S(\omega)$   | 19 |
| <b>II. Engineering quantum circuits</b>                   | 3  | 3. Noise spectroscopy  | 21 |
| A. From quantum harmonic oscillator to the transmon qubit | 3  | E. Engineering noise mitigation  | 21 |
| B. Qubit Hamiltonian engineering                          | 6  | 1. Materials and fabrication improvements  | 21 |
| 1. Tunable qubit: split transmon                          | 6  | 2. Design improvements   | 21 |
| 2. Towards larger anharmonicity: flux qubit and fluxonium | 7  | 3. Dynamical error suppression   | 22 |
| C. Interaction Hamiltonian engineering                    | 9  | 4. Cryogenic engineering   | 22 |
| 1. Physical coupling: capacitive and inductive            | 9  | <b>IV. Qubit control</b>   | 22 |
| 2. Coupling axis: transverse and longitudinal             | 10 | A. Boolean logic gates used in classical computers                               | 22 |
| <b>III. Noise, decoherence, and error mitigation</b>      | 11 | B. Quantum logic gates used in quantum computers                                 | 23 |
| A. Types of noise   | 11 | C. Comparing classical and quantum gates   | 26 |
| 1. Systematic noise                                       | 12 | 1. Gate sets and gate synthesis  | 26 |
| 2. Stochastic noise                                       | 12 | 2. Addressing superconducting qubits   | 27 |
| 3. Noise strength and qubit susceptibility                | 12 | D. Single-qubit gates  | 27 |
| B. Modeling noise and decoherence                         | 12 | 1. Capacitive coupling for X,Y control   | 27 |
| 1. Bloch sphere representation                            | 12 | 2. Virtual Z gate  | 29 |
| 2. Bloch-Redfield model of decoherence                    | 13 | 3. The DRAG scheme   | 30 |
| 3. Modification due to $1/f$ -type noise                  | 16 | E. The $i$ SWAP two-qubit gate in tunable qubits                                 | 31 |
| 4. Noise power spectral density (PSD)                     | 17 | 1. Deriving the $i$ SWAP unitary   | 31 |
| C. Common examples of noise                               | 17 | 2. Applications of the $i$ SWAP gate   | 32 |
| 1. Charge noise   | 17 | F. The CPHASE two-qubit gate in tunable qubits                                   | 32 |
| 2. Magnetic flux noise                                    | 18 | 1. Trajectory design for the CPHASE gate   | 34 |
| 3. Photon number fluctuations                             | 18 | 2. The CPHASE gate for quantum error correction                                  | 34 |
| 4. Quasiparticles   | 18 | 3. Quantum simulation and algorithm demonstrations using CPHASE                  | 35 |
| D. Operator form of qubit-environment interaction         | 19 | G. Two-qubit gates using only microwaves   | 36 |
|   |    | 1. The operational principle of the CR gate                                      | 36 |
|   |    | 2. Improvements to the CR gate and quantum error correction experiments using CR | 37 |
|   |    | 3. Quantum simulation and algorithm demonstrations with the CR gate              | 37 |

<sup>†</sup>philipk@mit.edu, <sup>‡</sup>william.oliver@mit.edu

# Equations of Motion in the Interaction Picture

- Let us express the Hamiltonian as a sum of two terms, the larger of which is time independent and for which solutions are known, and a smaller perturbation that contains all of the time dependence:  $H = H_0 + V(t)$

- In the Schrodinger picture:  $i\hbar\partial_t |\psi(t)\rangle_S = H |\psi(t)\rangle_S$

- The transformation for the state vector into the Interaction picture:

$$|\psi(t)\rangle_I = e^{iH_0 t/\hbar} |\psi(t)\rangle_S$$

- Equation of motion:

$$\begin{aligned} i\hbar\partial_t |\psi(t)\rangle_I &= i\hbar\partial_t \left( e^{iH_0 t/\hbar} |\psi(t)\rangle_S \right) \\ &= e^{iH_0 t/\hbar} (i\hbar\partial_t - H_0) |\psi(t)\rangle_S \\ &= e^{iH_0 t/\hbar} (H_0 + V - H_0) |\psi(t)\rangle_S \end{aligned}$$

$$\begin{aligned} i\hbar\partial_t |\psi(t)\rangle_I &= e^{iH_0 t/\hbar} V |\psi(t)\rangle_S \\ &= \underbrace{e^{iH_0 t/\hbar} V e^{-iH_0 t/\hbar}}_{V_I(t)} \underbrace{e^{iH_0 t/\hbar} |\psi(t)\rangle_S}_{|\psi(t)\rangle_I} \end{aligned}$$

- Only depends on time-dependent perturbation:

$$\boxed{i\hbar\partial_t |\psi(t)\rangle_I = V_I(t) |\psi(t)\rangle_I}$$

# Solution to Equation of Motion

- Construct an interaction picture solution by adding up eigenstates of the unperturbed Hamiltonian but with time-dependent coefficients:

$$|\psi(t)\rangle_I = \sum_n c_n(t) |n\rangle$$

- Substitute into equation of motion:

$$i\hbar \partial_t \sum_n c_n |n\rangle = e^{iH_0 t/\hbar} V e^{-iH_0 t/\hbar} \sum_n c_n |n\rangle$$

$$i\hbar \sum_n \dot{c}_n |n\rangle = e^{iH_0 t/\hbar} V \sum_n c_n e^{-iE_n t/\hbar} |n\rangle$$

$$i\hbar \sum_n \dot{c}_n \underbrace{\langle m | n \rangle}_{\delta_{mn}} = \underbrace{\langle m | e^{iH_0 t/\hbar} V}_{\langle m | e^{iE_m t/\hbar}} \sum_n c_n e^{-iE_n t/\hbar} |n\rangle$$

$$i\hbar \dot{c}_m = \sum_n V_{mn} e^{i\omega_{mn} t} c_n,$$

$$V_{mn} = \langle m | V | n \rangle, \quad \omega_{mn} = (E_m - E_n) / \hbar = -\omega_{nm}$$

# Application to 2-Level System

- Recall:  $H = \frac{1}{2}(E_1 + E_2)\sigma_0 + \frac{1}{2}(E_1 - E_2)\sigma_z + V\sigma_x$
- Choose zero of energy as the average, and  $V$  caused by sinusoidal RF signal:

$$H = -\frac{1}{2}\hbar\omega_{21}\sigma_z + V_0 \cos(\omega^{rf}t + \phi)\sigma_x$$

- Equations of motion  $i\hbar\dot{c}_n = \sum_n V_{mn} e^{i\omega_{mn}t} c_n$  become:

$$i\hbar\dot{c}_1 = V_0 \cos(\omega^{rf}t + \phi) e^{i\omega_1 t} c_2$$

$$i\hbar\dot{c}_2 = V_0 \cos(\omega^{rf}t + \phi) e^{i\omega_2 t} c_1$$

$$i\hbar\dot{c}_1 = \frac{V_0}{2} \left( e^{i(\omega^{rf}t + \phi)} + e^{-i(\omega^{rf}t + \phi)} \right) e^{-i\omega_2 t} c_2$$

$$i\hbar\dot{c}_2 = \frac{V_0}{2} \left( e^{i(\omega^{rf}t + \phi)} + e^{-i(\omega^{rf}t + \phi)} \right) e^{i\omega_2 t} c_1$$

# Solution in the Rotating Wave Approximation

- Assume the energy associated with the RF frequency is close to the transition energy between the two states:  $\omega^{rf} = \omega_{21} + \Delta$ ,  $|\Delta| \ll \omega_{21}$
- Then keep only the low-frequency components to the solution (Rotating Wave Approximation):

$$i\hbar\dot{c}_1 = \frac{V_0}{2} e^{i(\omega^{rf} - \omega_{21})t + i\phi} c_2 = \frac{V_0}{2} e^{i\Delta t + i\phi} c_2$$

$$i\hbar\dot{c}_2 = \frac{V_0}{2} e^{-i(\omega^{rf} - \omega_{21})t - i\phi} c_1 = \frac{V_0}{2} e^{-i\Delta t - i\phi} c_1$$

- Substituting the first equation into the second gives a second-order Diff. Equation for  $c_1$ :

$$\ddot{c}_1 - i\Delta\dot{c}_1 + \left(\frac{V_0}{2\hbar}\right)^2 c_1 = 0$$

- If the system starts off in state 1, then it is easily verified that the solution is

$$c_1(t) = A e^{i\Delta/2} \cos(\Omega t / 2)$$

$$c_2(t) = i \frac{2A\hbar}{V_0} e^{-i\Delta/2 - i\phi} \left( i \frac{\Delta}{2} \cos(\Omega t / 2) - \frac{\Omega}{2} \sin(\Omega t / 2) \right)$$

$$\Omega = \sqrt{\Delta^2 + \left(\frac{V_0}{\hbar}\right)^2}$$

$$|c_1|^2 + |c_2|^2 = 1 \Rightarrow A = \left(1 + (\Delta\hbar / V_0)^2\right)^{-1/2}$$

# Interaction Picture Calculation

## Driving at Resonance: Rabi Oscillations

- Calculate the 2 states RF driving frequency (See Appendix)
- If the RF driving frequency corresponds to the energy difference between the two states, then

$$\Delta = 0, \quad \omega^{rf} = \omega_{21}$$

- The coefficients then become

$$c_1(t) = \cos(\Omega_R t / 2)$$

$$c_2(t) = -ie^{-i\phi} \sin(\Omega_R t / 2)$$

$$\Omega_R = V_0 / \hbar$$

- Let state 1 correspond to the ground state, and state 2 to the excited state. The probability of finding the system in each state is given by

$$|c_g(t)|^2 = (\cos(\Omega_R t / 2))^2 = \frac{1}{2}(1 + \cos \Omega_R t)$$

$$|c_e(t)|^2 = (\sin(\Omega_R t / 2))^2 = \frac{1}{2}(1 - \cos \Omega_R t)$$

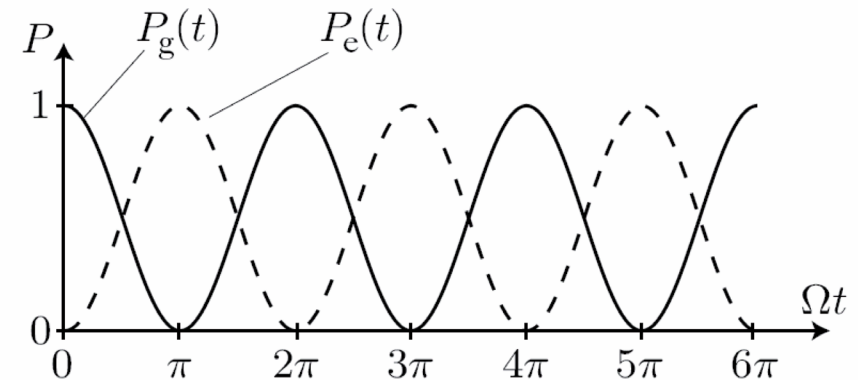


Figure 51: Time evolution of the probability  $P_g(t)$  and  $P_e(t)$  to find the atom in the ground (solid) and excited (dashed) state, respectively. [from D.A. Steck *Quantum and Atom Optics*]